

**MULTIGENIC ETIOLOGY OF HYPOPLASTIC LEFT HEART SYNDROME**  
**INSIGHTS FROM A NOVEL MOUSE MODEL**

by

**Shazina Saeed**

MBBS, Tribhuvan University, Nepal, 2006

MPH, University of Pittsburgh, 2011

Submitted to the Graduate Faculty of

Department of Human Genetics

Graduate School of Public Health in partial fulfillment

of the requirements for the degree of

Master of Science

University of Pittsburgh

2014

UNIVERSITY OF PITTSBURGH

Graduate School of Public Health

This thesis was presented

by

**Shazina Saeed**

It was defended on

January 27, 2014

and approved by

**Thesis Advisor:**

Cecilia Lo, PhD  
Professor and Chair  
Department of Developmental Biology  
School of Medicine  
University of Pittsburgh

**Committee Member:**

M. Ilyas Kamboh, PhD  
Professor  
Department of Human Genetics  
Graduate School of Public Health  
University of Pittsburgh

**Committee Member:**

Robert E. Ferrell, PhD  
Professor  
Department of Human Genetics  
Graduate School of Public Health  
University of Pittsburgh

Copyright © by Shazina Saeed

2014

Cecilia Lo, PhD

**MULTIGENIC ETIOLOGY OF HYPOPLASTIC LEFT HEART SYNDROME  
INSIGHTS FROM A NOVEL MOUSE MODEL**

Shazina Saeed, MS

University of Pittsburgh, 2014

**ABSTRACT**

Hypoplastic left heart syndrome (HLHS) is a complex congenital heart defect characterized by severe hypoplasia of the left ventricle (LV) along with stenosis/atresia of the aortic and mitral valves. HLHS patients show an incidence of 4-9 in 100,000 live births. Clinical studies have indicated that HLHS is a complex disease that is heritable, but no specific gene(s) have been identified. Despite the recent surgical advancements in the treatment of HLHS, understanding the developmental and genetic mechanisms associated with HLHS have proved to be a challenge due to the lack of an animal model.

In our study, we recovered 7 mutant mouse lines with HLHS from a large-scale recessive genetic screen with ENU mutagenesis. Further analysis of one HLHS mutant line, *Ohia*, showed that the HLHS phenotype is indeed heritable. Whole exome sequencing of two *Ohia* HLHS mutants revealed both were homozygous for mutations in five genes: Prolidase, NAD synthetase, Protocadherin a9, Sin3A-associated polypeptide 130 and N-acetyltransferase-ESCO1. GO term and KEGG ontology analysis of RNAseq data from heart tissue of E13.5, E14.5 and E18.5 *Ohia* mutants and littermate controls showed down-regulation of many genes involved in mitochondrial dysfunction, such as oxidative phosphorylation, Parkinson's, and Alzheimer's disease. Genes involved in pathways of cancer, extracellular matrix-receptor interaction, focal

adhesion, TGF-beta signaling, and Wnt signaling showed up regulation. These pathway enrichments are similar to results previously shown with microarray transcript profiling of human HLHS heart tissue.

In conclusion, we have generated the first mouse model for HLHS and showed it closely mirror not only the structural heart defect but also the metabolic changes seen in human HLHS patients. Using this mouse HLHS model, we will be able to interrogate the developmental pathways and molecular etiology underlying HLHS. Dissecting these elements would prove to be of immense public health significance, as despite the medical advances, every year 4-9 children in 100,000 live births are born with HLHS, and very few make it to adulthood. HLHS is universally fatal with 90% of deaths occurring in the first month of life in the absence of surgical treatment.

## TABLE OF CONTENTS

|   |            |
|---|------------|
| <b>PREFACE.....</b>   | <b>XII</b> |
| <b>1.0 INTRODUCTION.....</b>                                  | <b>1</b>   |
| <b>1.1 CONGENITAL HEART DEFECTS .....</b>                     | <b>1</b>   |
| <b>1.2 HYPOPLASTIC LEFT HEART SYNDROME .....</b>              | <b>3</b>   |
| <b>1.3 HYPOPLASTIC LEFT HEART SYNDROME HUMAN STUDIES.....</b> | <b>4</b>   |
| <b>1.4 GENETICS OF LEFT VENTRICULAR HYPOPLASIA.....</b>       | <b>7</b>   |
| <b>1.5 INTRODUCTION TO ENU MUTAGENESIS.....</b>               | <b>9</b>   |
| <b>2.0 METHODS AND MATERIALS .....</b>                        | <b>11</b>  |
| <b>2.1 ULTRASOUND IMAGING AND DOPPLER ECHOCARDIOGRAPHY .</b>  | <b>11</b>  |
| <b>2.2 NECROPSY, MICRO CT IMAGING AND HISTOPATHOLOGY</b>      |            |
| <b>EXAMINATIONS .....</b>                                     | <b>11</b>  |
| <b>2.3 DNA ISLOLATION .....</b>                               | <b>12</b>  |
| <b>2.4 EXOME SEQUENCING .....</b>                             | <b>13</b>  |
| <b>2.5 GENOTYPING .....</b>                                   | <b>14</b>  |
| <b>2.6 RNA EXTRACTIONS, REVERSE TRANSCRIPTION.....</b>        | <b>15</b>  |
| <b>2.7 BIOINFORMATICS ANALYSIS.....</b>                       | <b>15</b>  |
| <b>2.8 PATHWAY ANALYSIS VALIDATION BY REAL TIME PCR.....</b>  | <b>15</b>  |
| <b>2.9 IMMUNOSTAINING.....</b>                                | <b>16</b>  |

|            |   |           |
|------------|---|-----------|
| <b>3.0</b> | <b>RESULTS .....</b>  | <b>18</b> |
| <b>3.1</b> | <b>RECOVERY AND ANALYSIS OF HLHS MOUSE MODEL .....</b>  | <b>18</b> |
| <b>3.2</b> | <b>CARDIOMYOCYTE PROLIFERATION IS INCREASED IN HLHS.....</b>  | <b>20</b> |
| <b>3.3</b> | <b>INCREASED APOPTOSIS AND CARDIOMYOCYTE SIZE IN HLHS...</b>  | <b>22</b> |
| <b>3.4</b> | <b>TRANSCRIPTOME PROFILING OF HLHS MUTANTS SHOWS<br/>PERTURBATIONS IN MITOCHONDRIAL AND CELL SIGNALING PATHWAYS<br/>.....</b> | <b>24</b> |
| <b>3.5</b> | <b>RECOVERY OF MUTATIONS IN <i>OH1A</i> MUTANT LINE.....</b>  | <b>34</b> |
| <b>4.0</b> | <b>DISCUSSION .....</b>   | <b>40</b> |
| <b>5.0</b> | <b>CONCLUSION.....</b>  | <b>42</b> |
|            | <b>BIBLIOGRAPHY .....</b>   | <b>43</b> |

## LIST OF TABLES

|   |    |
|---|----|
| Table 1. List of primers used for genotyping of HLHS mouse line .....   | 14 |
| Table 2. List of Real-Time primers used for validation of RNAseq transcriptome profiling. ....                | 16 |
| Table 3. Whole exome sequencing of <i>Ohia</i> mutants revealed five mutations on chromosome 18<br>and 7..... | 35 |



## LIST OF FIGURES

|  |    |
|--|----|
| Figure 1. Adult Health and the Structures that are affected by CHD. ....   | 2  |
| Figure 2. Hypoplastic Left Heart Syndrome Heart Structure. ....  | 3  |
| Figure 3. Pathway analysis of human studies .....  | 6  |
| Figure 4. ENU mouse recessive mutagenesis and breeding scheme. ....  | 10 |
| Figure 5. Workflow of ENU screening in the Lo lab .....  | 12 |
| Figure 6. Whole Exome Sequencing Analysis Workflow. ....   | 13 |
| Figure 7. List of CHD seen clinically that were observed in our screen. ....   | 18 |
| Figure 8. Six independent mouse lines with HLHS models that were recovered in our ENU screen. ....   | 19 |
| Figure 9. HLHS mutants in line <i>Ohia</i> .....   | 20 |
| Figure 10. Increased expression of Phospho-histone H3 (Ph3) in the left ventricles of HLHS mutant hearts in line <i>Ohia</i> . ....  | 21 |
| Figure 11. Graphs representing increased cardiomyocyte proliferation in left ventricle of <i>Ohia</i> mutants at E14.5, E15.5, E16.5 and newborn (P0) developmental stages. .... | 22 |
| Figure 12. TUNEL staining of <i>Ohia</i> mutants shows increased apoptosis (arrows) in the left ventricle when compared to the control. ....                                     | 23 |

|  |    |
|--|----|
| Figure 13. Graphs representing increased apoptosis in Ohia mutants at developmental stages of E14.5, E15.5, E16.5 and newborn (P0).....                    | 23 |
| Figure 14. Increase in cardiomyocyte nuclear size in HLHS left ventricle at E16.5 and newborn mutants.....   | 24 |
| Figure 15. Multi-dimensional scaling (MDS) plot for HLHS samples .....   | 25 |
| Figure 16. Heat map of top 100 differentially expressed (DE) genes, showing the segregation on HLHS samples separately from their littermate controls..... | 26 |
| Figure 17. Pathway enrichments in up and down regulated genes in HLHS mutants.....   | 27 |
| Figure 18. Genes enriched in the pathways of cancer. ....  | 28 |
| Figure 19. Transcriptome profiling and pathway analysis of HLHS LV and RV tissue.....  | 29 |
| Figure 20. Upregulation of BMP4, VEGFA and TGFB2 in the LV of HLHS mutants in line <i>Ohia</i> .....   | 30 |
| Figure 21. Up regulation of WNT9B, FGF11 and COL2A1 in the LV of HLHS mutants in line <i>Ohia</i> .....  | 31 |
| Figure 22. Up regulation of FN1, ITGAV and ITGB5 in the LV of HLHS mutants in line <i>Ohia</i> .<br>.....  | 32 |
| Figure 23. Down regulation of COX8A, COX5B and BRP44L in the LV of HLHS mutants in line <i>Ohia</i> .....  | 33 |
| Figure 24. Highlighted in red are KEGG pathways and biological processes which overlap between our analysis and Ricci et al 2012. ....                     | 34 |
| Figure 25. Gel picture of Sap130 spliceforms in homozygous animals harvested at E12.5. Homozygous animals show missing wild type band. ....                | 36 |
| Figure 26. Spliceform 1 of Sap130 shows 76 bp insertion in intron 10. ....   | 36 |

|  |    |
|--|----|
| Figure 27. Spliceform 2 in Sap130 shows in frame mutation with deletion of exon 10 (105bps)                                    | 37 |
| Figure 28. Spliceform 3 in Sap130 shows skipping on exon 9 and 10. ....  | 37 |
| Figure 29. Summary of three spliceforms of Sap130 in line Ohia. Spliceform 1 and 3 result in premature truncated protein. .... | 38 |
| Figure 30. Genotypes of 15 HLHS mutants and 8 HLH mutants. Decision tree analysis of HLHS mutants with ROC=0.085. ....         | 39 |

## **PREFACE**

I would like to take this opportunity to thank the people who made my research experience possible. Thank you Dr. Cecilia Lo for allowing me the chance to work in your lab and for helping me to become a more mature researcher. I would also like to thank Dr.Xiaoqin Liu and Brian Gibbs without whose help this project would not have been possible. Thank you Dr.Hisato Yagi, Dr.Rama Darmela, Dr.Maliha Zahid, Dr. Cheng Cui and Dr.You Li for your help and guidance throughout my project. You have not only guided me, but have also been a great motivation and inspiration. Dr.Abha Bais and Dr.Dennis Kostka, a very special thank you for helping me understand bioinformatics and for always being there to answer my questions. Thank you, George Gabriel and Ruby Slabicki, for making all this analysis happen and for always being there for supporting and motivating me. I would also like thanking the rest of the Lo lab for your tremendous support.

I would also like to thank the members of my thesis committee, Dr. Robert Ferrell and Dr. Ilyas Kamboh for taking time out of their busy schedules to provide me critical feedback on my thesis as well as presentation.

I would also like to thank my friends, family and specially my husband for their continuous support throughout my time away from home. Your support, encouragement and motivation kept me going.

## **1.0 INTRODUCTION**

### **1.1 CONGENITAL HEART DEFECTS**

Congenital heart defects (CHD) are the most common type of birth defect. They affect 8 out of every 1,000 newborns. Each year, more than 35,000 babies in the United States are born with congenital heart defects [NIH, 2011]. CHD are an important cause of childhood morbidity and mortality worldwide [Bruneau BG, 2008]. Despite recent advances in medical and surgical care, the etiology of CHD is yet to be elucidated. Studies such as the Baltimore-Washington Infant Study have found that CHD is multifactorial, with both genetic and environmental contributing factors. [Ferencz C. et al 1993]. Gene targeting has aided in the generation of a several mouse models with cardiac developmental defects. Studies like these have led to the identification of multiple transcriptional regulators, structural genes and signaling molecules that are critical for normal cardiac development [Ashleigh A Richards et al, 2010].

CHD are often associated with a wide variation of phenotypes, making them a complex disorder with complex underlying mechanisms. The genetic etiology has thus been difficult to determine. CHD have a limited correlation between the genetic mutation and the specific phenotype. Some reasons underlying the complexity of CHD include: genetic heterogeneity in which similar cardiac defects are caused by more than one genetic mutation [Benson 2000]; variable expressivity in which one gene may cause multiple phenotypes [Benson 2000]; reduced

penetrance where a person may be a carrier for the disease-causing mutation but not express the CHD phenotype [Benson 1998]; one or more causative genes for CHD associated with chromosomal alterations [Momma 1995]; single gene defects with or without the expression of the CHD phenotype [McElhinney 2002] .

Congenital heart diseases affect most parts of the heart (Fig. 1). CHD can be classified into three broad categories; cyanotic heart disease, left-sided obstruction defects and septation defects. Left-sided obstructive lesions, the second main type of congenital heart disease, include hypoplastic left heart syndrome (HLHS), mitral stenosis, aortic stenosis, aortic coarctation and interrupted aortic arch (IAA) [Bruneau BG, 2008].

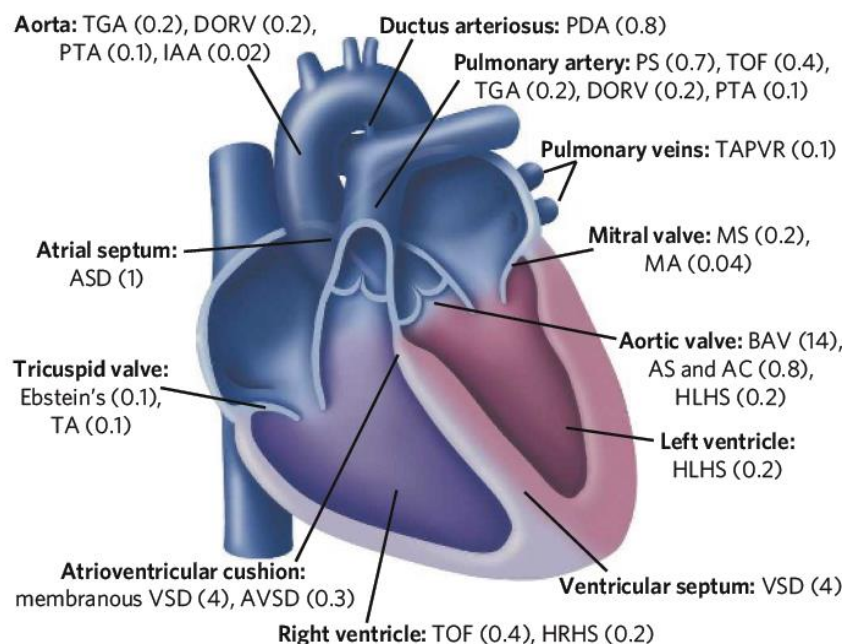


**Figure 1. Adult Health and the Structures that are affected by CHD.**

AC, aortic coarctation; AS, aortic stenosis; ASD, atrial septal defect; AVSD, atrioventricular septal defect; BAV, bicuspid aortic valve; DORV, double outlet right ventricle; Ebstein's, Ebstein's anomaly of the tricuspid valve; HLHS, hypoplastic left heart syndrome; HRHS, hypoplastic right heart; IAA, interrupted aortic arch; MA, mitral atresia; MS, mitral stenosis; PDA, patent ductus arteriosus; PS, pulmonary artery stenosis; PTA, persistent truncus arteriosus; TA, tricuspid atresia; TAPVR, total anomalous pulmonary venous return; TGA, transposition of the great arteries; TOF, tetralogy of Fallot; VSD, ventricular septal defect. [Bruneau BG, 2008]

## 1.2 HYPOPLASTIC LEFT HEART SYNDROME

Hypoplastic left heart syndrome (HLHS, OMIM: #241550) (Fig. 2) is characterized by abnormally developed atrial septum and a severe underdevelopment of the left side of the heart, including hypoplasia of the left ventricle, aortic atresia/ stenosis and mitral valve atresia/ stenosis. [Madhu Gupta et. al 2008]

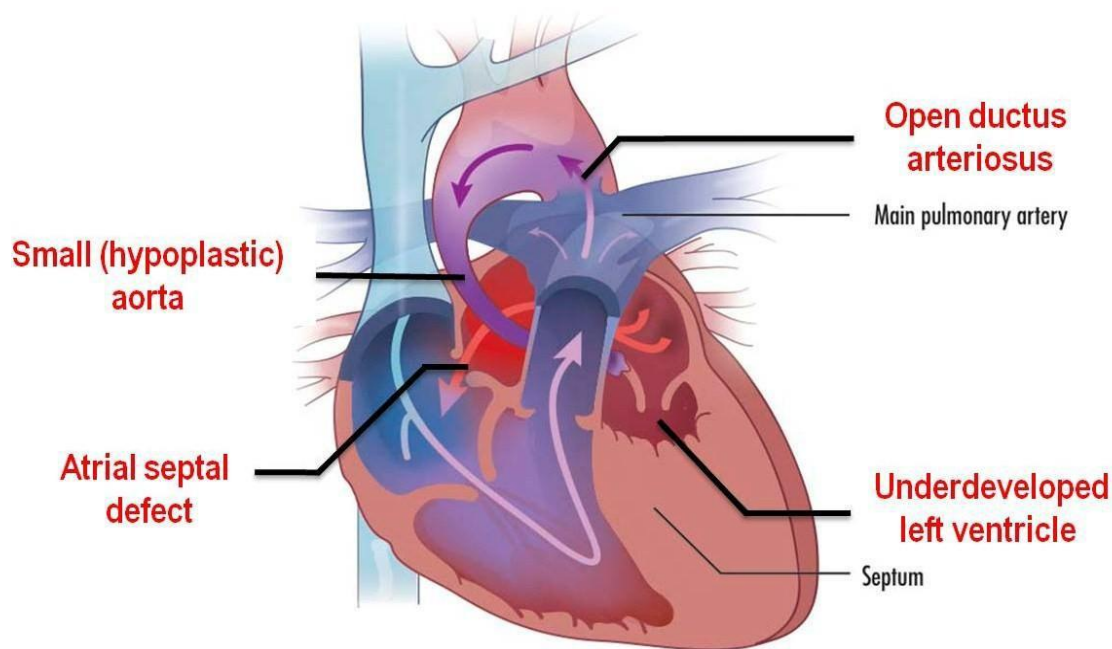


**Figure 2. Hypoplastic Left Heart Syndrome Heart Structure.**

The four main defects are shown; patent ductus arteriosus, hypoplastic left ventricle, atrial septal defect and hypoplastic aorta. Blood flow indicated by direction of arrows.

<http://www.childrenshospital.org/az/Site502/mainpageS502P0.html>

This rare disorder occurs in about 0.16-0.36 of every 1,000 live births ([www.orpha.net](http://www.orpha.net)) and has a higher prevalence in males than females. HLHS comprises 1.2 -1.5% of all congenital heart defects (CHD) or 7-9% of all CHD diagnosed within the first year of life. Before surgical

treatment became available, HLHS was universally fatal with 90% of deaths occurring in the first month of life [ Gutgesell H.P. et al, 1995].

HLHS is one of the many CHDs where cardiac malformations are characterized by poor growth of cardiac chambers and major blood vessels, subsequently impairing organ perfusion and oxygenation. In HLHS, the poor development of the left-sided structures is likely to be due to an underlying genetic defect [Seema Mittal et.al, 2013] . At present the etiology or the molecular abnormalities in HLHS remain unknown. Currently no studies have shown a clear association of genetic factors to HLHS, however, a high incidence of CHD in the first degree relatives, suggesting an autosomal recessive mode of inheritance, and familial clustering as well as association with chromosomal abnormalities like Turner's syndrome, trisomies 13 and 18 ; and terminal deletion of 11q23-qter have been reported [Hinton RB et al, 2007; Sedmera D. et al, 2005; Shokeir MH et al, 1971; Madhu Gupta et al ,2008]. These reports collectively suggest a possible role of genetic factors in the etiology of HLHS. The aim of this study is to explore the genetics of HLHS through a novel mouse model and further perform functional studies to gain better understanding of the etiology of HLHS.

### **1.3 HYPOPLASTIC LEFT HEART SYNDROME HUMAN STUDIES**

Some interesting insights have helped us in understanding the etiology of HLHS. Almost all of these studies are based on findings from HLHS patients, as there has been no animal model for HLHS. In 2003, Teresa J Bohlmeier et al studied the heart tissue from patients with HLHS



using routine histology, immunohistochemistry. The HLHS hearts in her study showed disorganized muscle fibres, myocytes were smaller with scanty cytoplasm, and abundant connective tissues. [Teresa J Bohlmeier et al, 2003]

Hinton et al, 2007 conducted a study at Cincinnati Children's Hospital, to determine the heritability in families identified by a HLHS proband. A total of 38 probands with HLHS, a 3-generation family history was obtained and a total of 235 participants were recruited. They found the heritability of HLHS alone and with associated CVM was 99% and 74% ( $p < 0.00001$ ), respectively. The sibling recurrence risk for HLHS was 8%, and for CVM was 22%. The high heritability of HLHS as obtained from this study suggests that it is determined largely by genetic factors. Since the left- and right-sided valve dysplasia often co occurred in HLHS probands and the increased prevalence of bicuspid aortic valve (BAV) in family members suggested that HLHS is a severe form of valve malformation. [Hinton et al, 2007]

However, the genetic etiology or the molecular abnormalities in HLHS remain unknown. Madhu Gupta et al 2008 did a study to provide a comparative expression analysis of HLHS and non-HLHS hearts. Their comprehensive gene expression analysis of the atrial septum of HLHS and non-HLHS patients by microarray and identified chromatin remodeling, transcriptional regulation and cell cycle regulation to be altered in HLHS. Although this analysis proved to be very important in provided biological components that may be involved in HLHS, its limitation was in the fact if the findings from the atrial septum could be applied to the global effects of the left ventricle in HLHS. [Madhu Gupta et al 2008]

Ricci et al, 2012, studied the right ventricle (RV) of six neonates with HLHS and compared it to the RV and left ventricle (LV) from non-diseased control subjects using a genome-wide exon array analysis to determine differentially expressed genes and alternatively

spliced transcripts. In HLHS, over 180 genes were differentially expressed and 1800 were differentially spliced, resulting in changes in a variety of biological processes involving cell metabolism, cell adherence and cytoskeleton. (Fig 3) [Ricci et al, 2012]

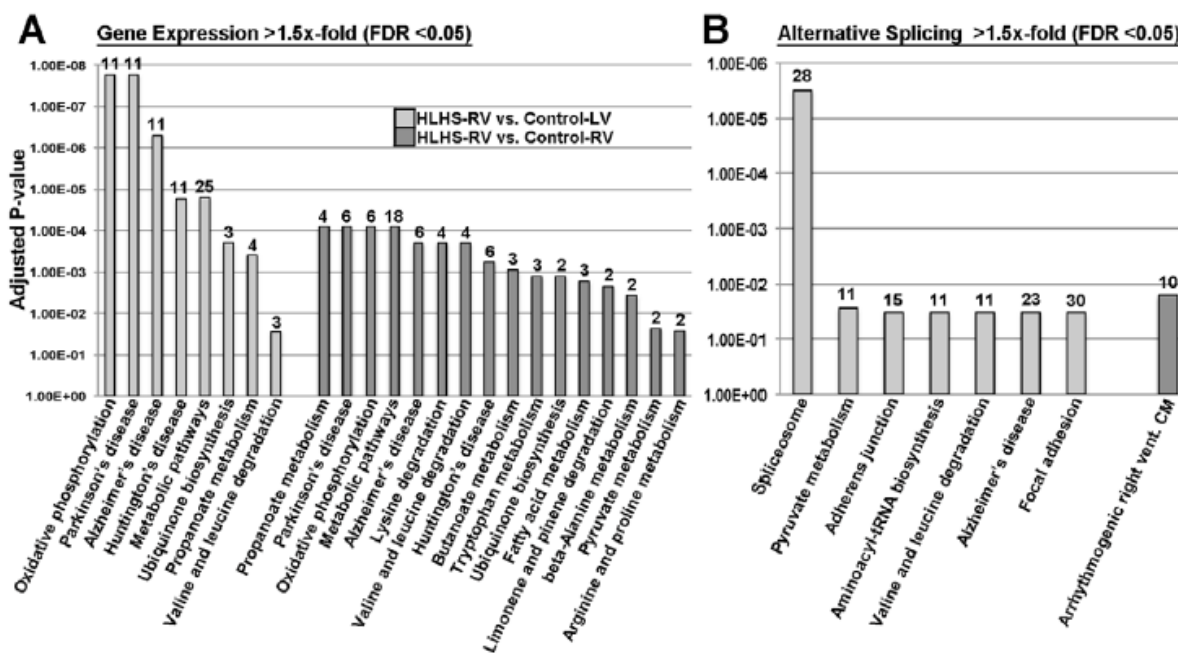


Figure 3. Pathway analysis of human studies.

KEGG pathway analysis to show the relative significance of affected biological processes in HLHS-RV samples versus controls as a result of differential gene expression and alternative splicing events. Numbers indicate the number of differentially expressed or alternatively spliced transcripts that within each indicated KEGG category. [Ricci et al 2012]

In 2013, Seema Mittal et al, for the first time did a study on human fetuses at LV and right ventricle (RV) paired myocardial samples were obtained from 32 second-trimester fetuses with HLHS. Their results suggest that the fetal LV in HLHS undergoes reprogramming with decrease in cardiac lineages and increase in fibroblast lineages. This process involves TGFB 1 up-

regulation, DNA damage, premature cell senescence, and loss of DNA replication association with impaired cardiac differentiation and vasculogenesis. [Seema Mittal et al. 2013]

The results from these studies have been very exciting and important discoveries in the understanding the etiology of HLHS. However, to gain a detailed insight into its genetics and treatment options would only be possible in the presence of an animal model.

## **1.4 GENETICS OF LEFT VENTRICULAR HYPOPLASIA**

In elucidating the genetics of HLHS, a question important to address is why HLHS is a LV specific phenotype. It is thus crucial to understand the genetics of LV development and hypoplasia.

LV hypoplasia describes a lethal congenital heart abnormality that usually occurs in association with obstruction to LV outflow. [Edward.J.Hickey et al 2012]. The majority of cases of LV hypoplasia occur in association with downstream obstruction, which in most cases is aortic stenosis. Therefore, it has been suggested that LV hypoplasia is predominantly a disease of the aortic valve [Hinton et al 2007]. But the discoveries of 2 basic helix-loop-helix transcription factors—HAND-1 and HAND-2, which appear central to early ventricular development, suggest that in some cases, the primary defect is in the ventricle itself.

During initial development of the heart tube, HAND expression is almost uniform, in both the ventricles, but marked differences in expression are then seen in the craniocaudal axis in a ventricle-specific fashion [Srivastava et al. 1999]. *HAND-1* transcripts are expressed in the conus arteriosus, truncus arteriosus, primitive atrium, and primitive ventricle, but their expression is significantly deficient in the bulbus cordis, which is the future right ventricle. ON

the other hand, *HAND-2* is predominantly expressed in the bulbus cordis. It can therefore be inferred that mutations in *HAND-1* are associated with LV hypoplasia and abnormalities in LVOT development [Srivastava et al 1997].

Experiments have suggested that loss-of-function mutations result in non-viable fetuses due to lack of development of the left and right ventricles. Some gene-sequencing studies of human hearts affected by LV hypoplasia have recently demonstrated loss-of-function mutations in *HAND-1* in a large proportion [Edward.J.Hickey et al 2012].

Apart from the *HAND* genes, the T-box (*Tbx*) genes are also important in cardiovascular development. Persistent overexpression of *Tbx5* results in heart looping defects, abnormalities of early chamber development and loss of ventricular-specific gene expression, indicating an essential role for *Tbx5* in early heart development [Horb and Thomsen, 1999; Hatcher et al., 2001; Liberatore et al., 2000]. Studies have shown that *Tbx5* expression is restricted to the atria and the left ventricle. Hence, *Tbx5* would provide a novel and valuable marker to explore the mechanism of LV hypoplasia [Bruneau et al., 1999; Yamada et al., 2000]. In the chick and mouse hearts *Tbx5* is expressed ubiquitously, the ventricular walls are thinner than normal, and the trabecular formation is coarse and rough. These phenotypic changes indicate that *Tbx5* regulates cardiac muscle differentiation [J.K Takeuchi et al 2003].

*Tbx5* protein associates and interacts physically with the cardiac homeoprotein *Nkx2.5*, which is important for cardiac muscle development (Bruneau et al., 2001; Hiroi et al., 2001). Interactions between *Tbx5* and *GATA4* activate the atrial natriuretic factor (ANF) promoter. These studies support that *Tbx5* plays multiple roles and changes in its protein level in differentiating cardiomyocytes might affect the transcriptional control of cardiac genes by disturbing the balance of these multiple interactions. Both the loss and gain of *Tbx5* function

disturb the transcriptional control of Tbx5 targets, probably through the abnormal balance between the Tbx5, Tbx20, GATA4 and Nkx2.5 proteins [Edward.J.Hickey et al 2012].

Although, the above mentioned findings have aided us in our understanding of the genetic basis of LV hypoplasia, the lack of an animal model, makes it difficult for us to analyze the changes in development of LV in HLHS hearts.

## **1.5 INTRODUCTION TO ENU MUTAGENESIS**

Lack of an animal model for HLHS has been a limiting factor to further interrogate the genetic and molecular basis of its etiology. The phenotype-based forward genetic approach that is carried out on the LoLab serves as an excellent avenue to identify important genes based on their mutant phenotype; hence all biases based on protein structures, gene expression patterns, or knowledge on their homologues in other species is excluded.

N -Ethyl- N - Nitrosourea (ENU) is a powerful alkylating agent that generates single nucleotide substitutions (both transitions and transversions) in mouse spermatogonia at a frequency of one point mutation every 1 to 2 megabases throughout the genome [Kile 2005]. The single nucleotide mutations thus induced may simulate many human genetic conditions and serves as better disease models than the deletions and transgene insertions as a result of reverse genetic manipulation [Anderson KV. 2000]. Typically, C57BL/6J mice (G0) are ENU mutagenized and the resulting G1 males and their G2 daughters are backcrossed to generate G3 fetuses for ultrasound scanning to recover recessive mutations causing CHD. (Fig 4)

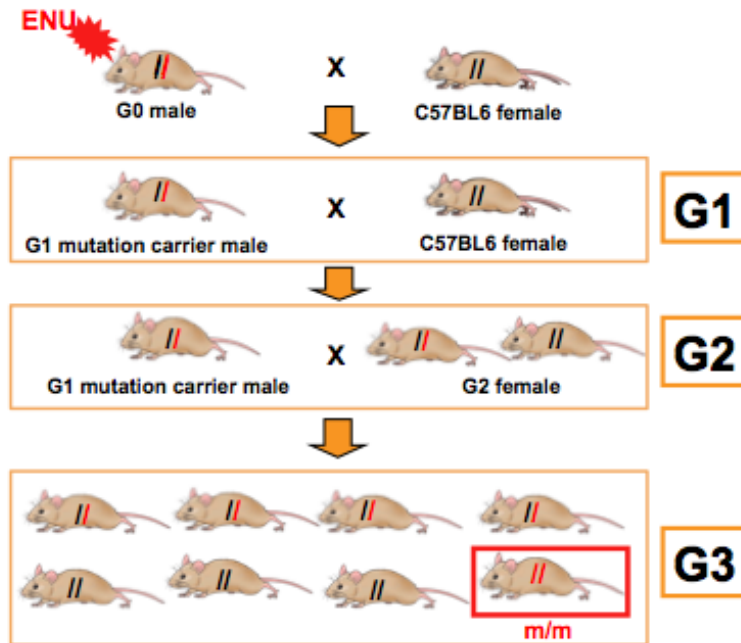


**Figure 4. ENU mouse recessive mutagenesis and breeding scheme.**

C57BL/6J mice (G0) are ENU mutagenized and the resulting G1 males and their G2 daughters are backcrossed to generate G3 fetuses for ultrasound scanning to recover recessive mutations causing congenital heart disease (CHD).

## **2.0 METHODS AND MATERIALS**

### **2.1 ULTRASOUND IMAGING AND DOPPLER ECHOCARDIOGRAPHY**

ENU mutagenized pregnant G2 females were sedated with isoflurane, and ultrasound scanned using the Acuson Sequoia C512 with a 15 MHz transducer. Litters with abnormal fetuses were then further scanned using the Vevo2100 UBM with 40MHz transducer for specific CHD diagnosis. (Fig 5)

### **2.2 NECROPSY, MICRO CT IMAGING AND HISTOPATHOLOGY EXAMINATIONS**

Fetuses or neonates were collected and fixed in 10% formalin, then examined by necropsy, micro-computed tomography (micro-CT) or magnetic resonance imaging (micro-MRI) and episcopic fluorescence image capture (EFIC) [Rosenthal J, ET AL 2004], a histopathology examination. EFIC served as the gold standard for CHD diagnosis. (Fig 5)

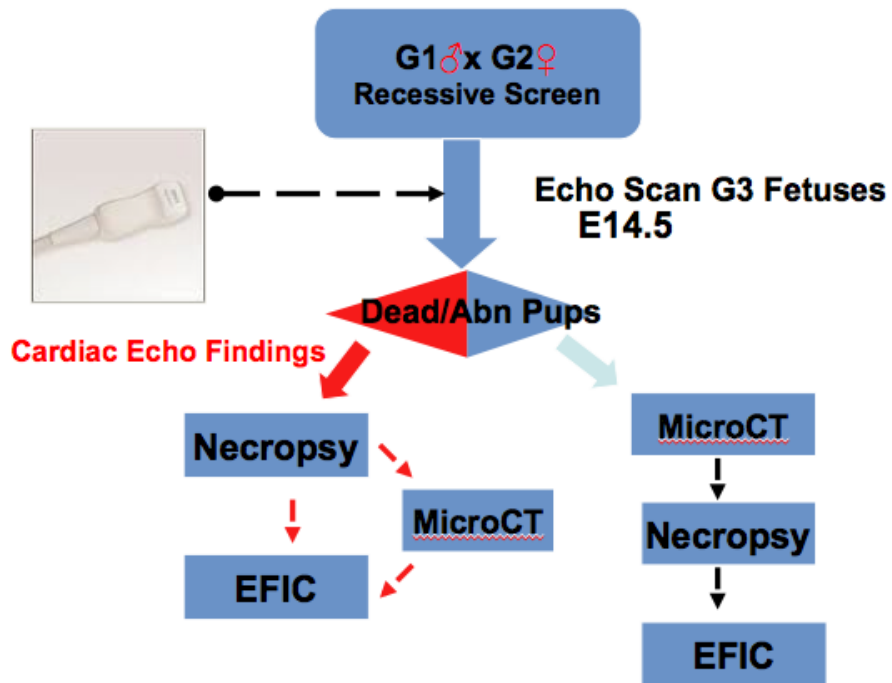


Figure 5. Workflow of ENU screening in the Lo lab.

*(Please note that this figure was adapted from a figure presented by Dr. Xiaoqin Liu in the Lo lab)*

### 2.3 DNA ISLOLATION

Skin samples collected from fetuses or neonates were snap frozen in liquid nitrogen and DNA was extracted using Gentre Pure genelysis buffer (QIAGEN), followed by DNA purification (QIAGEN). The DNA thus obtained was used for exome sequencing.



## 2.4 EXOME SEQUENCING

Two mutant mice from Family 635 were sequence captured using Agilent SureSelect Mouse All Exon kit, and sequenced using SOLiD 4 sequencer. Over 100x target coverage were achieved for each exome. Sequence reads were aligned to C57BL/6J mouse reference genome (mm9) and analyzed using LifeScope software (Life Technologies). Sequence variants were annotated with annovar (<http://www.openbioinformatics.org/annovar/>) and filtered against dbSNP128 and our in-house database with custom scripts. Novel homozygous coding variants present in both mouse exomes were identified as candidate disease causing mutations. (Fig 6)

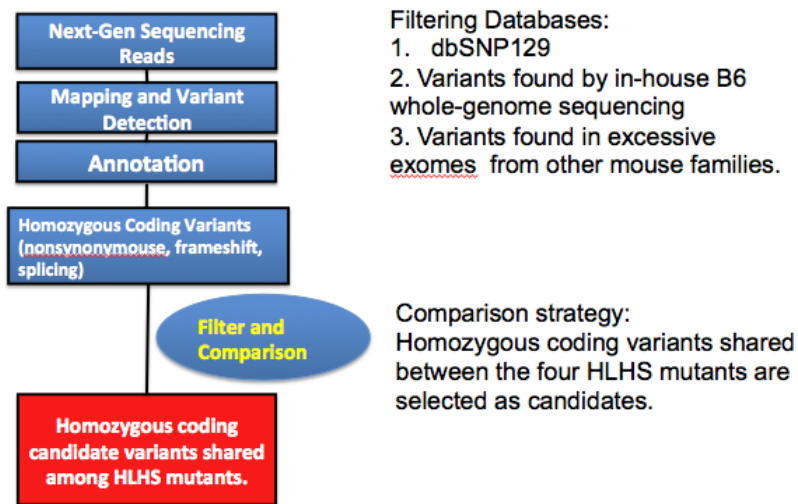


**Figure 6. Whole Exome Sequencing Analysis Workflow.**

*(Please note that this figure was adapted from a figure presented by Dr.You Li in the Lo lab)*

## 2.5 GENOTYPING

Tail snips from fetuses and neonates were lysed overnight using standard protocols. The DNA thus obtained was used for genotyping by PCR amplification using Roche PCR kit. Primers were designed using Primer3 (<http://primer3.ut.ee/>). List of primers used are provided in Table 1.

**Table 1. List of primers used for genotyping of HLHS mouse line.**

| <b>Primer Name</b> | <b>Forward Primer</b>   | <b>Reverse Primer</b>  |
|--------------------|-------------------------|------------------------|
| mG-Sap130          | TTTTTACCCTCTTTTCAGGATCT | AAGTCAAATTCAGAGTTGCTTG |
| mG-Pcdha9          | ACCTGATCATTTGCCATTTGC   | TCTGGGACACACATTTGTCAT  |
| mG-Pepd            | TAGCCCAGGCAGAGCTTA      | GCGGTGTCTGTCAGTCAA     |
| mG-NADsyn1         | ATGGGTACCCTGAAGCTCCT    | TCTCTTCAGCGGCTATGGAT   |
| mG-Escol           | AACAAGCCTGTTTCCCATGA    | TTGGGAAAAATTGAGGAAGAG  |

## **2.6 RNA EXTRACTIONS, REVERSE TRANSCRIPTION**

Total RNA from mouse embryos was isolated using RNeasy micro kit with on-column DNase I digestion method (QIAGEN). cDNA libraries were produced from RNA extracted by using High capacity RNA to cDNA kit (Applied Biosystems).

## **2.7 BIOINFORMATICS ANALYSIS**

EdgeR analysis was used for identifying differentially expressed genes. GO terms KEGG pathways were obtained using the DAVID (<http://david.abcc.ncifcrf.gov/chartReport.jsp>).

## **2.8 PATHWAY ANALYSIS VALIDATION BY REAL TIME PCR**

Real-time PCR was done using Applied Biosystem HT7900 with Power SYBR Green PCR Master Mix (Applied Biosystem) following standard protocol. *β-actin* gene, which is ubiquitously expressed, was used as an internal control. Primers were designed Roche Universal Probe Library. The Primer sequences are listed in Table 2.

**Table 2. List of Real-Time primers used for validation of RNAseq transcriptome profiling.**

| Primer name | Forward Primer           | Reverse Primer           |
|-------------|--------------------------|--------------------------|
| Bmp4        | gatctttaccggctccagtct    | tgggatgttctccagatgttc    |
| Tgfb2       | aggaggtttataaaatcgacatgc | tagaaagtgggcgggatg       |
| Vefga       | aaaaacgaaagcgcaagaaa     | tttctccgctctgaacaagg     |
| Cox8b       | ccagccaaaactcccactt      | gaaccatgaagccaacgac      |
| Cox5b       | ttaaatgaattgggaatctccac  | gtccttaggaagcccatcg      |
| Brp44l      | tgaatagccgagagtcctaaa    | tgatgaagacaaataaggttagca |
| Wnt9b       | ccaagagaggaagcaaggac     | tctcaggccgctcttcac       |
| Fgfl1       | tgccagaaacagctcctcat     | agtttggtgacgatgccttt     |
| Col2a1      | acccccaggtgctaattgg      | gaacacctttgggaccatctt    |
| Fn1         | cggagagagtgccectacta     | cgatatgtgtgaatcgcaga     |
| Itgav       | ggtgtggatcgagctgtctt     | caaggccagcatttacagtg     |
| Itgb5       | tttgccaagttccaaagtga     | tctgtacagggggtttgagg     |

## 2.9 IMMUNOSTAINING

Embryos were fixed overnight in 4% Paraformaldehyde, dehydrated through graded ethanol, and paraffin embedded. Sections were cut at 8 µm and mounted on Poly-Prep slides (Poly-L-lysine coated by Sigma). The antigens were retrieved by incubating in the 20XBulls eye decloaker (Biocare medical) for 40 minutes at 100 °C. The source and concentration of primary antibodies are: anti-Phospho-histone H3 (1:100 dilution) (Millipore,Ser10), anti-MF 20 (1:100 dilution) (Developmental Studies Hybridoma Bank), Further, sections were incubated with secondary antibody AF555-goatanti-rabbit IgG(1:000) and AF488 Goat anti-mouse IgG2b(1:1000), WGA

(1:200 dilution) (Developmental Studies Hybridoma Bank). AF-488 Donkey anti-goat IgG. Nuclei were stained with DAPI (1:5000). Coverslips were mounted using Vectashield (Vector laboratories, Inc). Terminal deoxynucleotidyltransferase-mediated dUTP-biotin nick end labeling (TUNEL) assays were performed using the Roche (Ref#12156792910) by following the manufacturer's recommendations. Sections were visualized under Olympus Confocal microscope. Quantitative analysis was performed on Nikon elements at Centre of biological imaging, University of Pittsburgh.

### 3.0 RESULTS

#### 3.1 RECOVERY AND ANALYSIS OF HLHS MOUSE MODEL

From ultrasound scanning over 60,000 fetuses thus far, most of the CHD found in the clinical setting were detected in our screening, including ventricular septal defects (VSD), Double outlet right ventricle (DORV), Persistent Truncus Arteriosus (PTA), Atrioventricular Septal Defects (ASD) to name a few. Detailed lists of CHDs recovered from our ENU screen is below.

#### 60,000 Fetuses Screened

|     |  |
|-----|--|
| 176 | Ventricular <u>Septal</u> Defect       |
| 75  | Double Outlet Right Ventricle          |
| 38  | Persistent <u>Truncus Arteriosus</u>   |
| 14  | Transposition of the Great Arteries    |
| 65  | <u>Atrioventricular Septal</u> Defects |
| 19  | Pulmonary Atresia                      |
| 14  | <u>Aortic Stenosis/Coarctation</u>     |
| 8   | Tricuspid Atresia                      |
| 15  | Hypoplastic Right Heart Syndrome       |

#### 7 Hypoplastic Left Heart Syndrome

Figure 7. List of CHD seen clinically that were observed in our screen.

We recovered 7 HLHS mutants after screening a total of 60,000 fetuses.  
*(Please note that this figure was adapted from a figure presented by Dr. Xiaoqin Liu in the Lo lab)*

The most novel among these findings was the recovery of 7 HLHS mutants in six independent mouse lines. This finding is indeed very exciting because prior to the recovery of our HLHS mouse model it was widely believed that HLHS could not be modeled in mice due to its short gestation period of only 20 days. Further analysis by necropsy followed by EFIC histology confirmed the diagnosis of HLHS. Which by definition includes the finding of LV hypoplasia, hypoplastic aorta, hypoplastic mitral valve, and absence of VSD. (Figure 8)

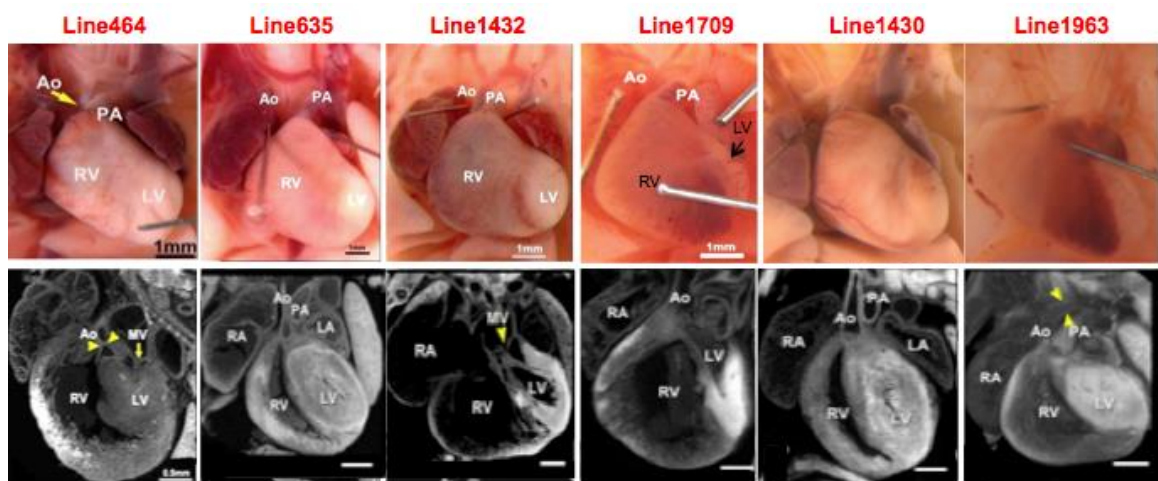


**Figure 8. Six independent mouse lines with HLHS models that were recovered in our ENU screen.**

*(Please note that this figure was adapted from a figure presented by Dr. Xiaoqin Liu in the Lo lab)*

Among these six lines we further bred line 635, where we had recovered two mutants from the original screen, named *Ohia* to recover more mutants to validate our HLHS model. It is interesting to note that our *Ohia* mutants exhibit craniofacial defects such as microcephaly, low set ears, proboscis, recessed or absent lower jaw. Craniofacial defects have also been documented in several HLHS patients [Aparna VP et. al 2013, Licht DJ et al 2009, Tracy A. Glauser et al 1990], suggesting a neurodevelopmental involvement in the pathophysiology of HLHS. (Fig 9) shows the classical phenotype of HLHS in *Ohia* mutants.

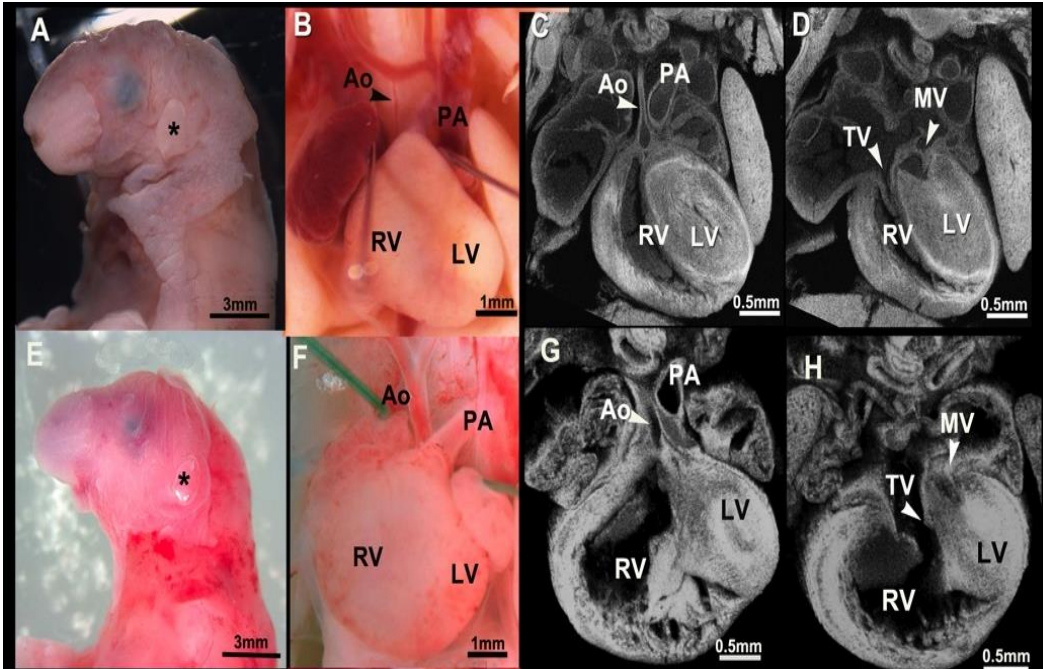


**Figure 9. HLHS mutants in line *Ohia*.**

HLHS mutants in line *Ohia* shows craniofacial defects with microcephaly, proboscis, low set ears (A, E), Necropsy images of HLHS hearts showing classical HLHS phenotype (B,F), which are confirmed by histopathology showing hypoplastic left ventricle (LV) , hypoplastic aorta, mitral valve atresia/stenosis (C,D,G,H).

### **3.2 CARDIOMYOCYTE PROLIFERATION IS INCREASED IN HLHS**

In order to determine whether cardiomyocytes proliferation was altered in HLHS mutants, hearts harvested from E14.5-E16.5 and P0 (newborn) mutants and their littermate controls were immunostained for Cell proliferation marker and cardiomyocyte marker (MF20). HLHS hearts demonstrated an increased cardiomyocyte proliferation on the left ventricle. Expression of phospho-histone H3 (pHH3), which relates to mitotic chromosomal condensation, was significantly higher in HLHS mutants compared to in littermate control. In separately analyzing



the LV vs the RV, it can be noticed that most of the difference between mutants and controls is accounted for by the significant differences in the LV alone between the two groups. (P-values at E14.5=0.0398, E15.5=0.2508, E16.5=0.0043,  $P_0=0.0225$ ).

Interestingly, increased cardiomyocyte proliferation was also observed on the right ventricle but it was not significantly different between controls and mutants. Taken together, this data demonstrates that left ventricle of HLHS mice in line *Ohia* have increased cardiomyocyte proliferation.

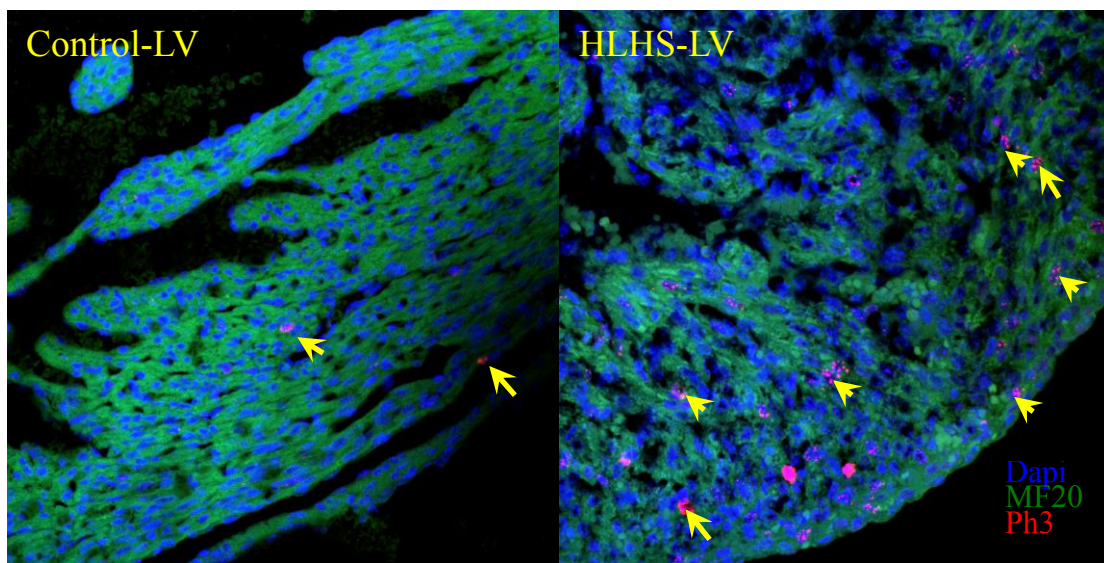


**Figure 10. Increased expression of Phospho-histone H3 (Ph3) in the left ventricles of HLHS mutant hearts in line *Ohia*.**

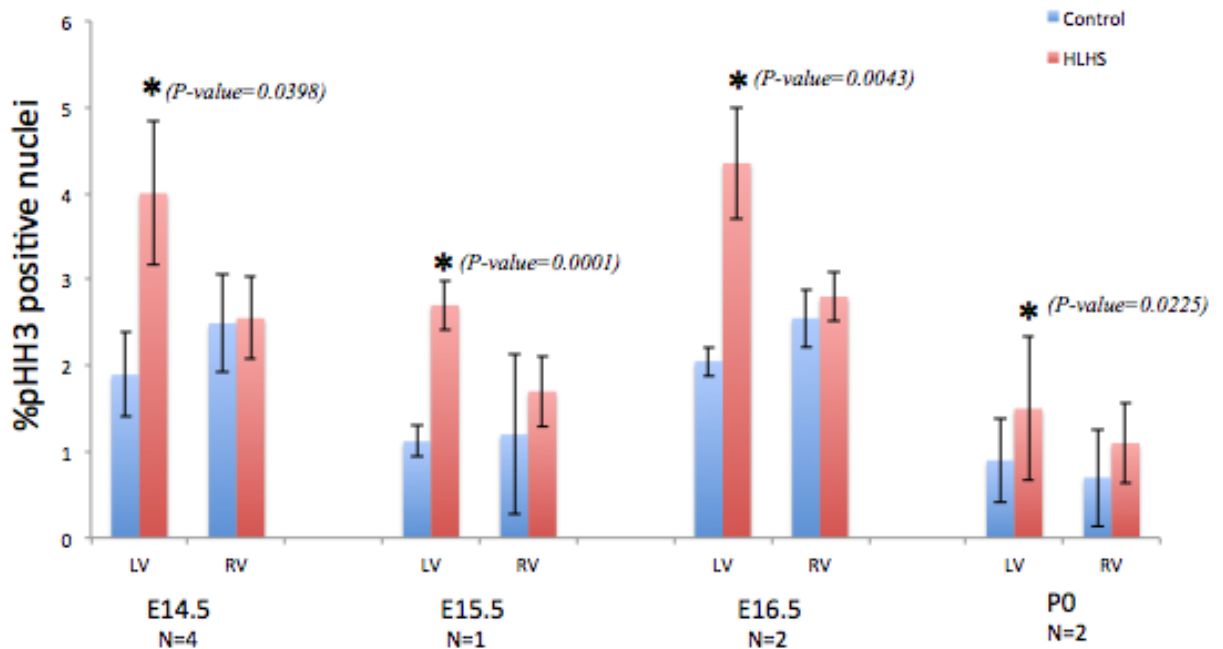


**Figure 11. Graphs representing increased cardiomyocyte proliferation in left ventricle of *Ohia* mutants at E14.5, E15.5, E16.5 and newborn (P0) developmental stages.**

### 3.3 INCREASED APOPTOSIS AND CARDIOMYOCYTE SIZE IN HLHS

TUNEL staining of hearts harvested at E14.5-E16.5 and P0 from HLHS mutants and littermate controls demonstrated an increase in apoptosis in HLHS mutant left ventricles in comparison to littermate controls. HLHS mutants had significantly higher percentage of apoptosis compared to in littermate controls. (P-value at E14.5=0.0001, E15.5=0.0209, E16.5=0.3012)

Cardiomyocyte size was measured to rule out hyperplasia versus hypertrophy of individual cardiomyocytes. Our data suggests that during later stages of development, there is an increase in the cardiomyocyte nuclear size in left ventricles of HLHS mutants in line *Ohia*.

(Figure 14)

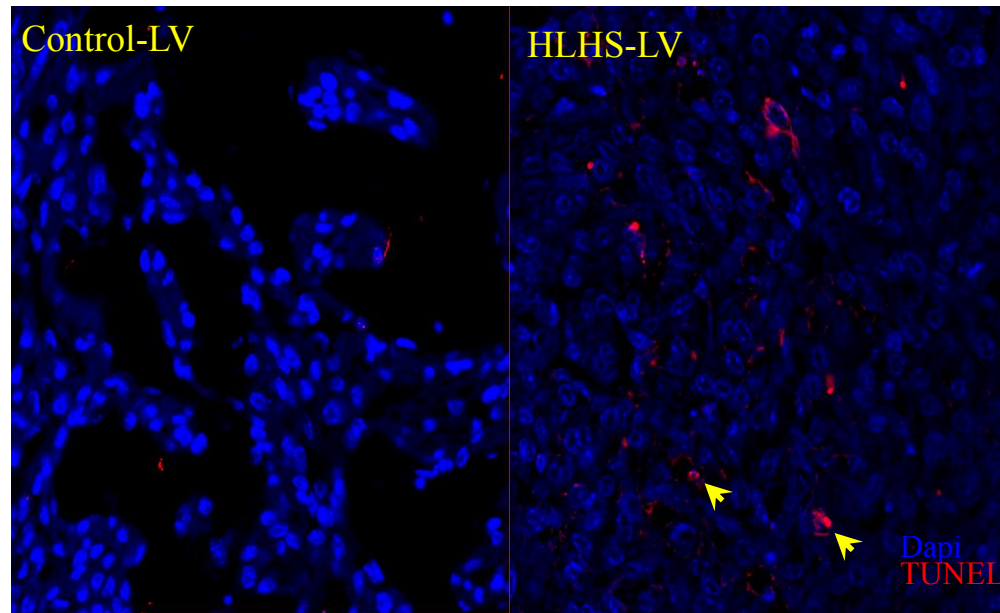


Figure 12. TUNEL staining of *Ohia* mutants shows increased apoptosis (arrows) in the left ventricle when compared to the control.

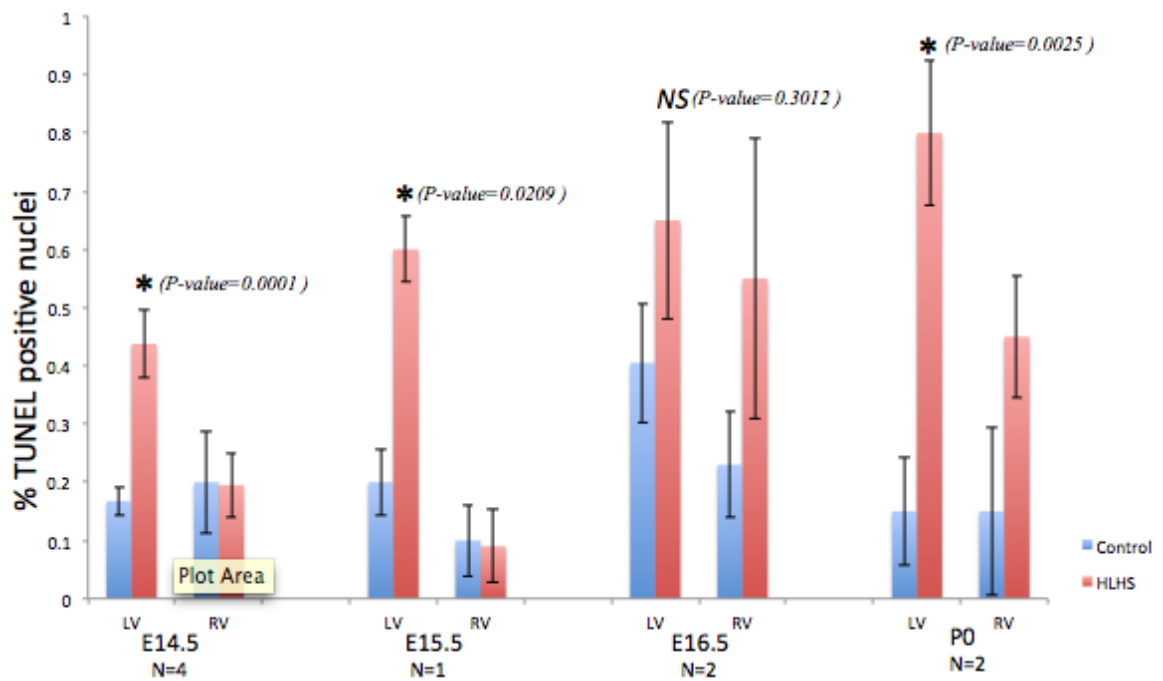
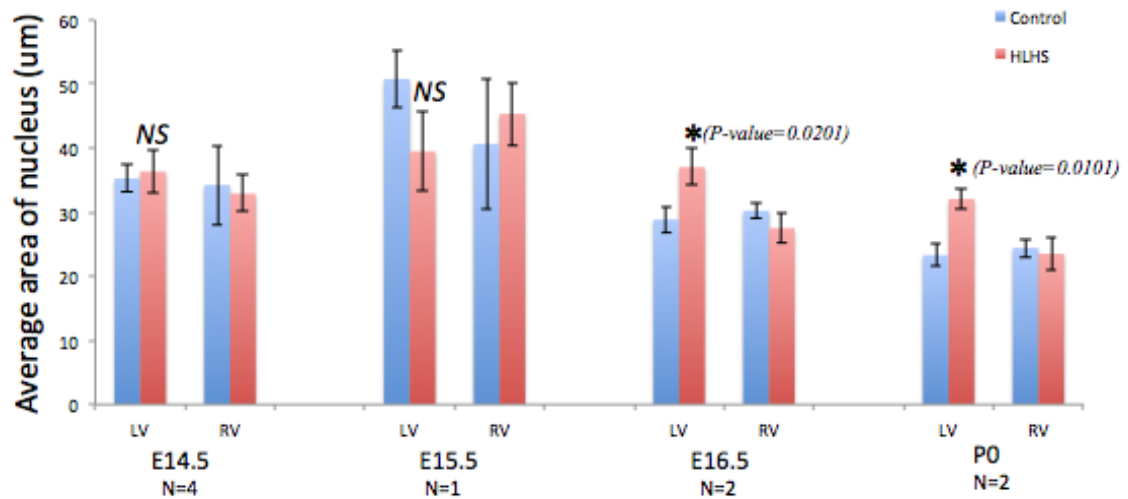


Figure 13. Graphs representing increased apoptosis in *Ohia* mutants at developmental stages of E14.5, E15.5, E16.5 and newborn (P0).



**Figure 14. Increase in cardiomyocyte nuclear size in HLHS left ventricle at E16.5 and newborn mutants.**

### **3.4 TRANSCRIPTOME PROFILING OF HLHS MUTANTS SHOWS PERTURBATIONS IN MITOCHONDRIAL AND CELL SIGNALING PATHWAYS**

To obtain a global view of gene expression in HLHS mutant hearts, we measured gene expression in E13.5, E14.5 and E18.5 heart tissues by RNA-seq. For the E13.5 samples we dissected the hearts into left and right ventricles separately. For E14.5 and E18.5 whole heart samples were used. A total of 4176 differentially expressed (DE) genes were obtained with a false discovery rate (FDR) of  $< 0.05$ . These 4176 genes were further categorized as up and down regulated genes in the HLHS mutants in comparison to their littermate controls, followed by pathway analysis using DAVID. The up regulated genes were enriched in pathways related to cancer, Focal adhesion, regulation of cytoskeleton, axon guidance, Wnt signaling, extracellular matrix and TGF-beta signaling (Figure 17). Down regulated genes involved in

Parkinson's, Alzheimer's and Huntington's diseases which are primarily genes related to mitochondrial function. Further, we performed Q-PCR experiments to validate some of the highly expressed genes (fold change >0.5) in enriched pathways.

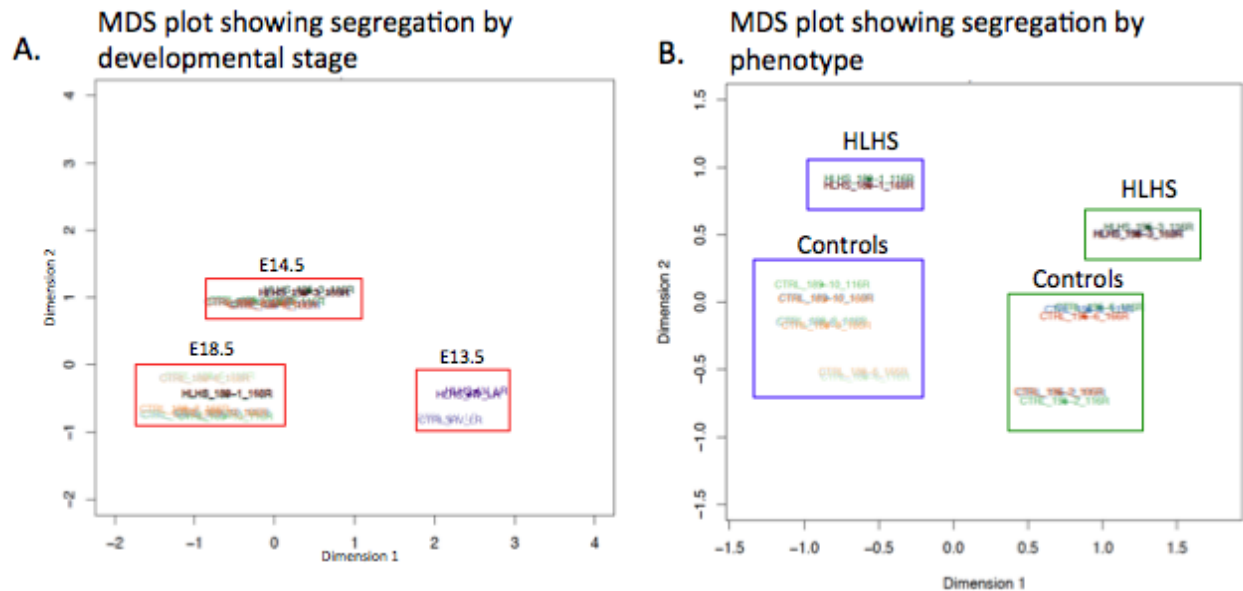


**Figure 15. Multi-dimensional scaling (MDS) plot for HLHS samples.**

Multi-dimensional scaling (MDS) plot for samples at E13.5, E14.5, and E18.5, segregated by developmental stages (A). (B) Shows a MDS plot for samples at E18.5 and E14.5 segregating by phenotype; HLHS or littermate controls.

## Heatmap: HLHS vs. CTRL

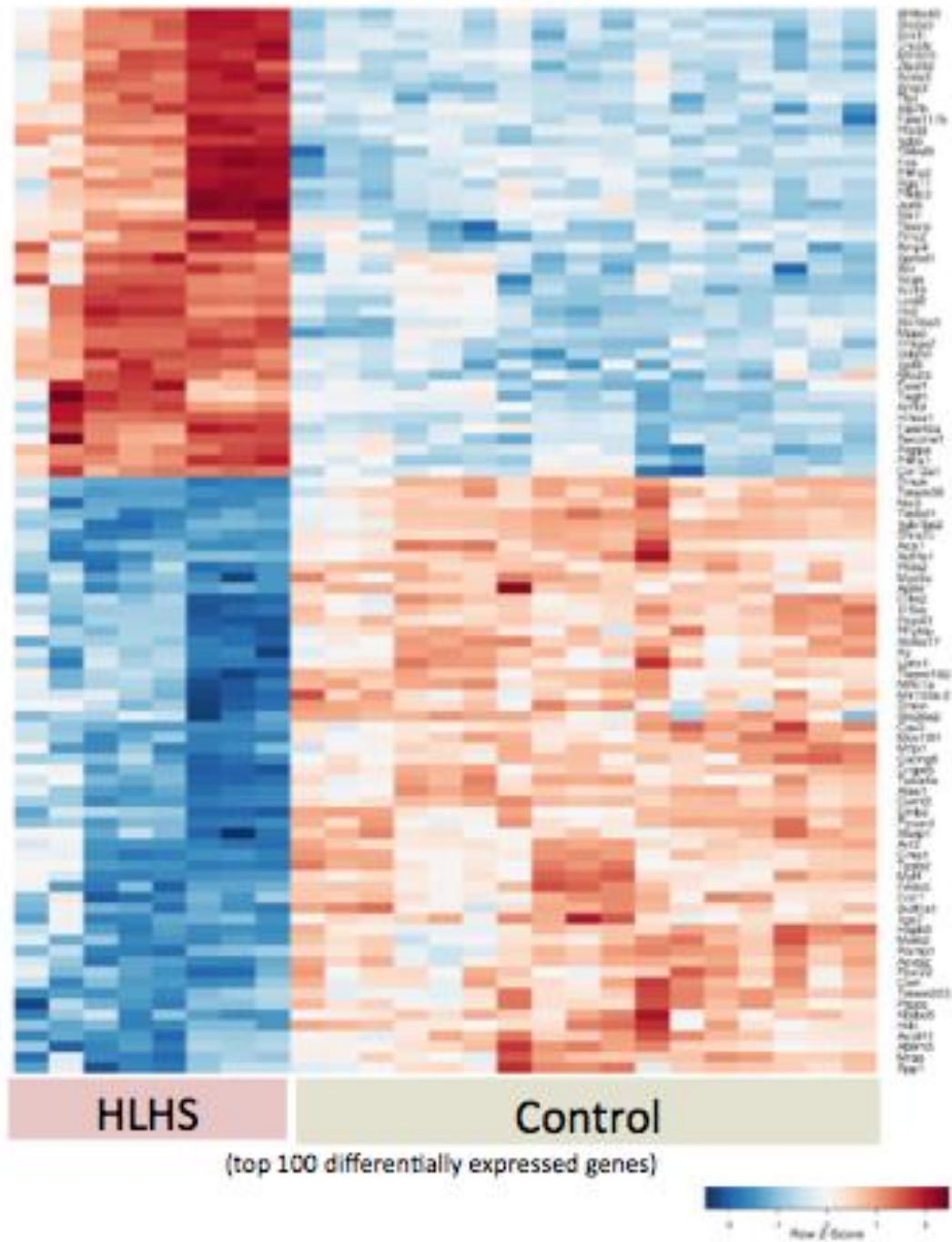
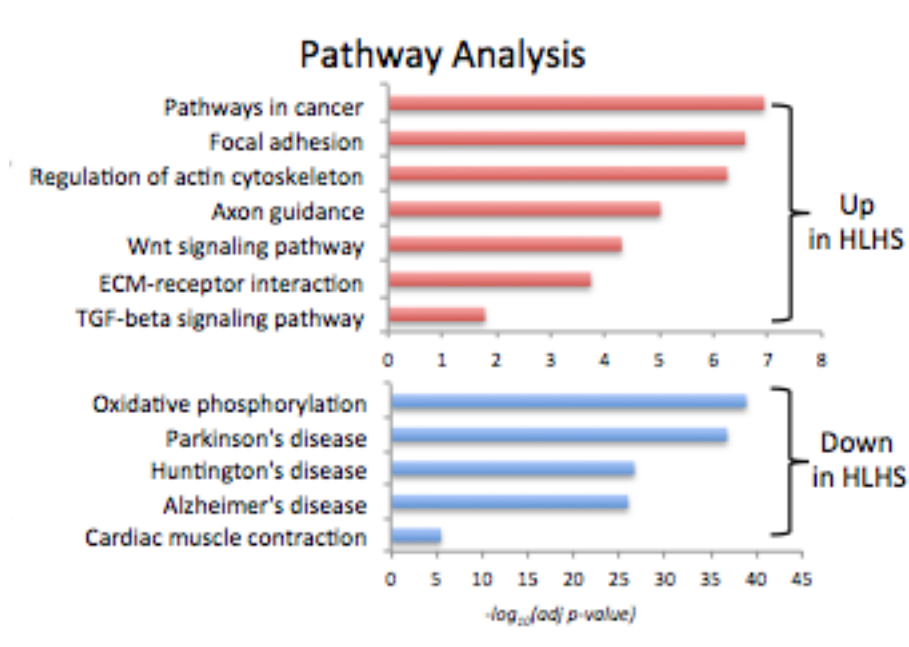


Figure 16. Heat map of top 100 differentially expressed (DE) genes, showing the segregation on HLHS samples separately from their littermate controls.





**Figure 17. Pathway enrichments in up and down regulated genes in HLHS mutants.**

Among the genes enriched in the pathways of cancer (total 74), several genes were involved in apoptosis and cell proliferation. There were integrins, genes from the TGFB super family, Wnt signaling, growth factors and transcription related genes. (Figure 18)

# Pathways of Cancer

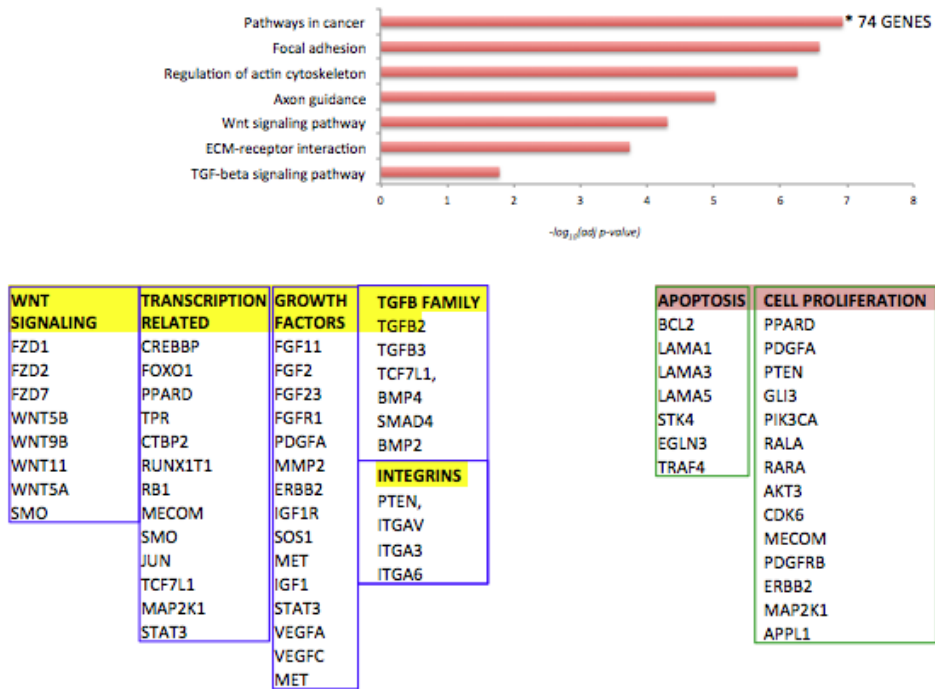
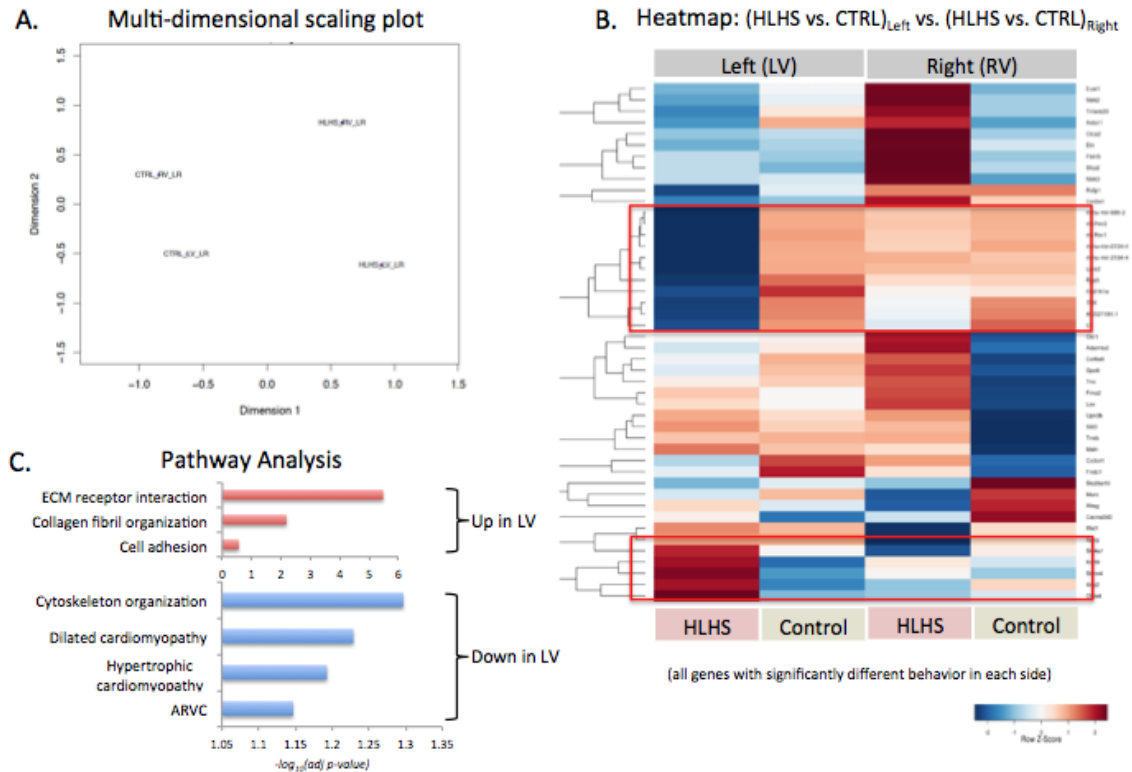


Figure 18. Genes enriched in the pathways of cancer.

Next we separately analyzed at the E13.5 samples, with RNA-seq results from left and right ventricle. We wanted to look at the transcriptome profiling of genes that behave differently not only in HLHS mutants and their littermate but also in the left versus right ventricles. This analysis yielded us 46 DE genes, showing perturbations in pathways related to cell adhesion, Extracellular matrix, collagen and cytoskeletal organization, dilated and hypertrophic cardiomyopathies. (Figure 19)





**Figure 19. Transcriptome profiling and pathway analysis of HLHS LV and RV tissue.**

(A) MDS plot showing the segregation of HLHS mutants and littermate controls based on side as well as phenotype. (B) Heat map showing the 46 DE genes that behave differently on the LV in comparison RV in both mutants and controls. (C) Pathway enrichments in up and down regulated DE genes in the left ventricle of HLHS mutants and their littermate controls.

Q-PCR experiments were performed for some DE genes in major pathways to compare their relative expressions on the LV versus the RV at stages E14.5 and E17.5. (Figure 20,21, 22 and 23). Some differences in expression could be accounted for by difference in developmental stages.

## Validation of up regulated pathways

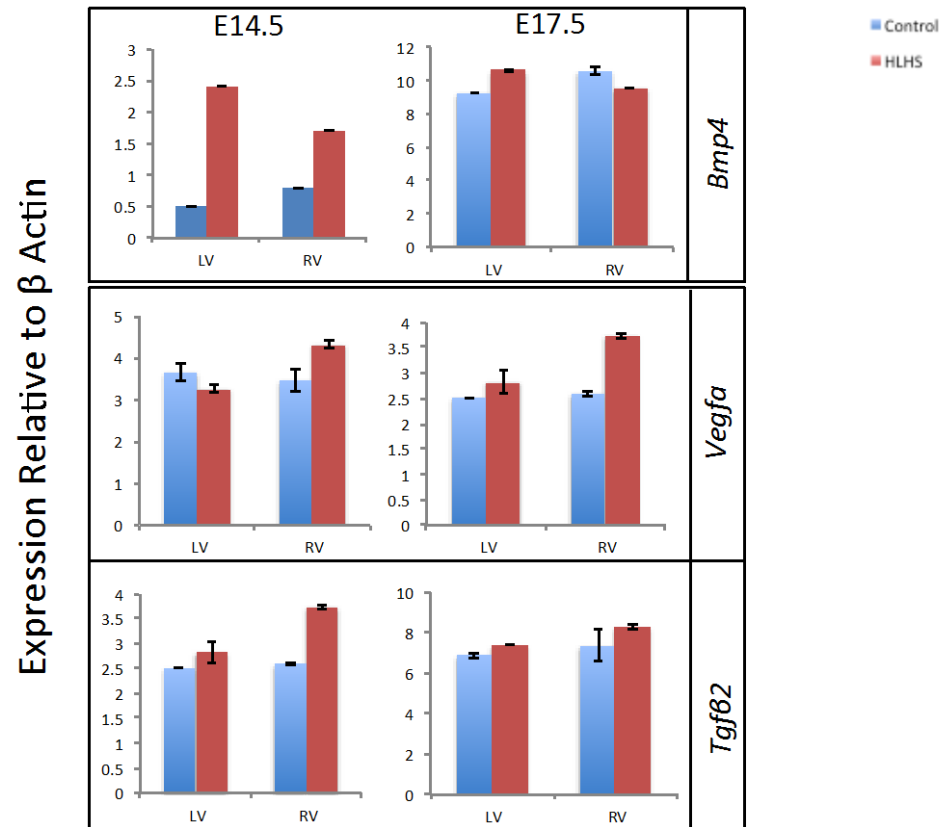


Figure 20. Upregulation of BMP4, VEGFA and TGFB2 in the LV of HLHS mutants in line *Ohia*.

## Validation of up regulated pathways

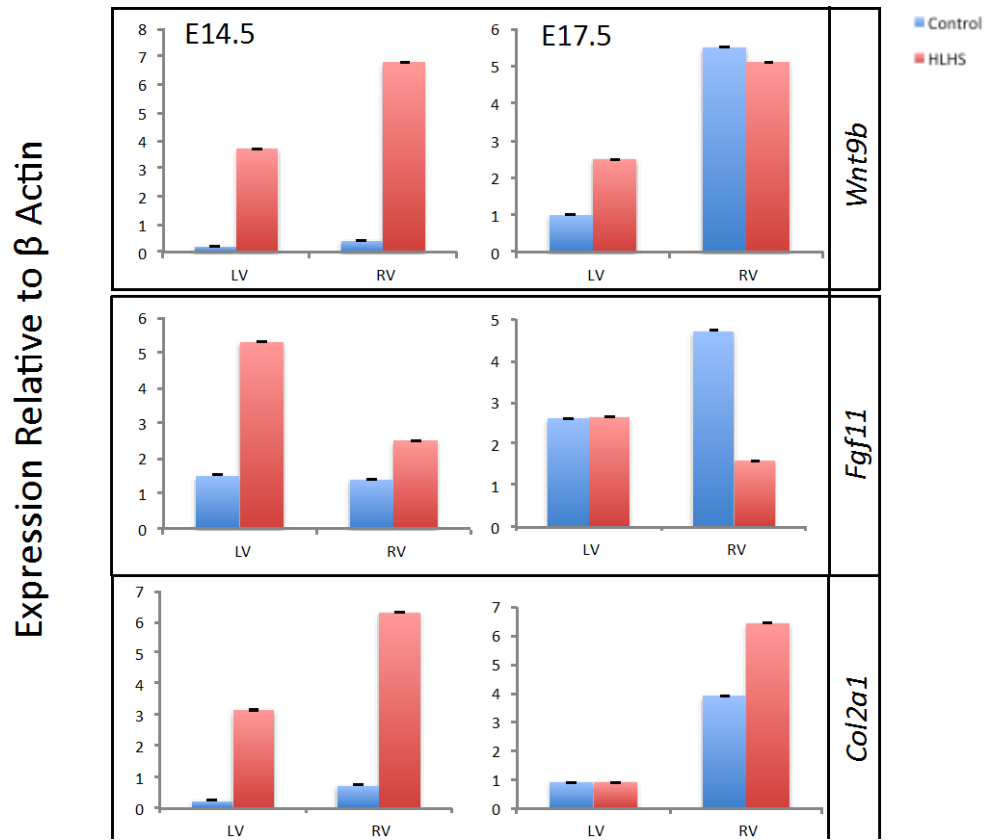


Figure 21. Up regulation of WNT9B, FGF11 and COL2A1 in the LV of HLHS mutants in line *Ohia*.

## Validation of up regulated pathways

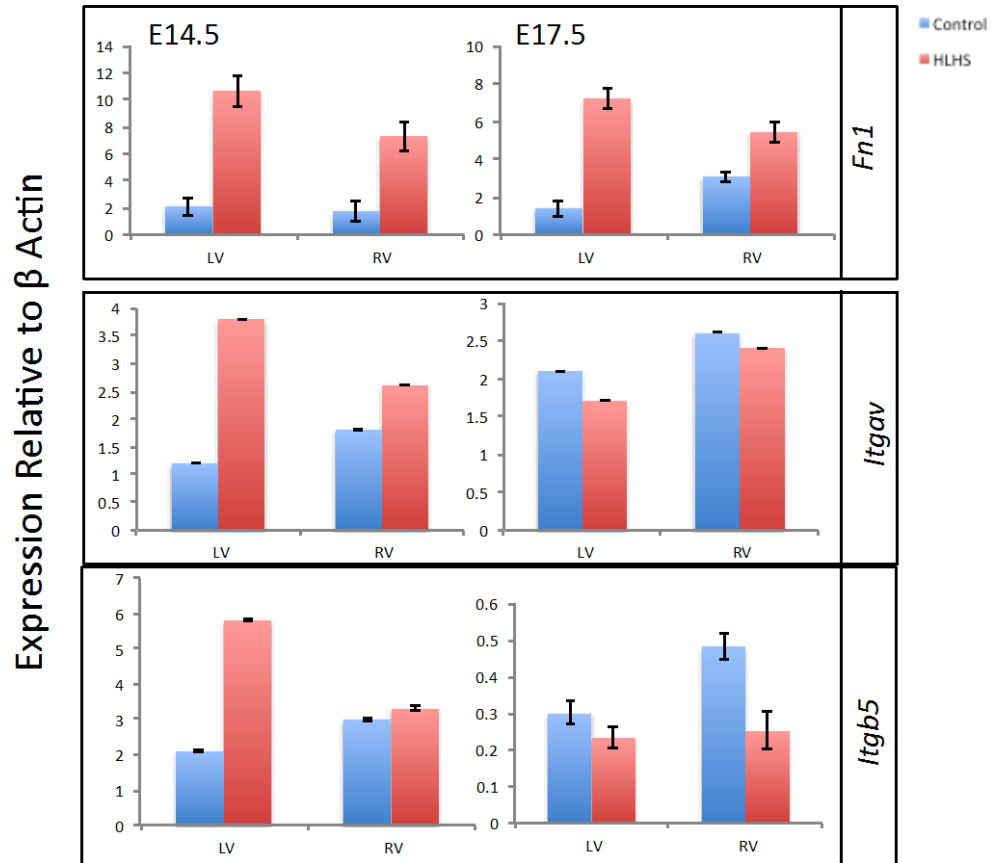


Figure 22. Up regulation of FN1, ITGAV and ITGB5 in the LV of HLHS mutants in line *Ohia*.

## Validation of down regulated pathways

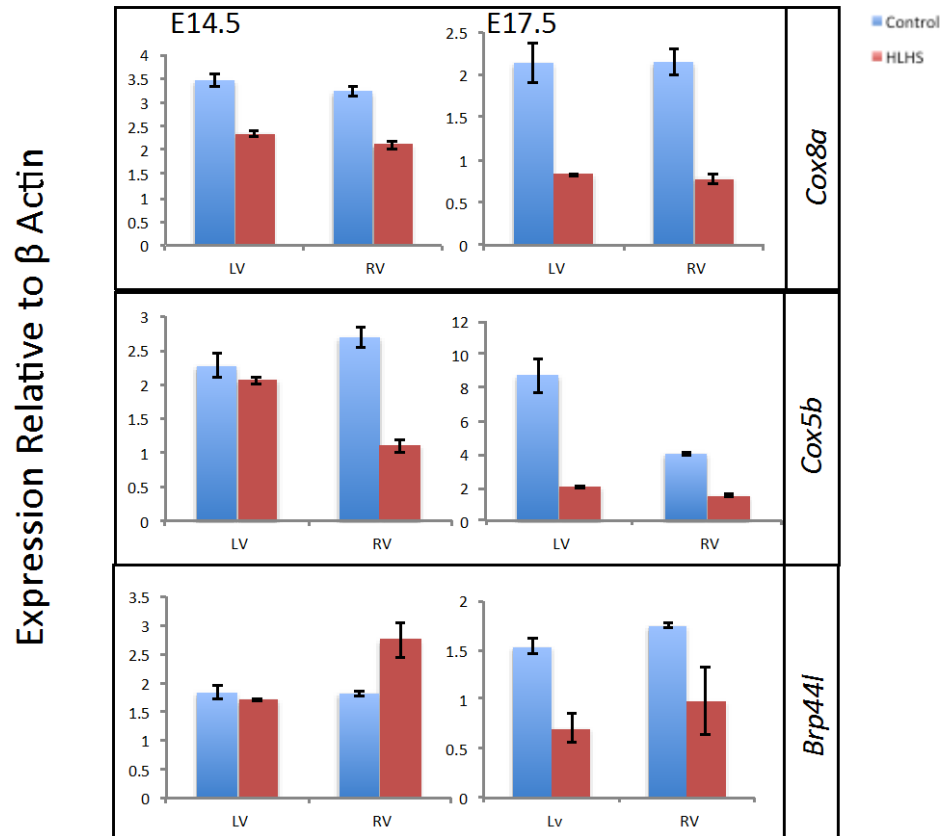


Figure 23. Down regulation of COX8A, COX5B and BRP44L in the LV of HLHS mutants in line *Ohia*.

All in all, our transcriptome profiling analysis, yielded us results that were strikingly similar to those obtained in Ricci et al 2012 stud, comparing HLHS RV to Control RV and LV. (Figure 24)



**Table 3.**Whole exome sequencing of *Ohia* mutants revealed five mutations on chromosome 18 and 7.

| Gene    | Chromosome | Protein  | Full name                             |
|---------|------------|----------|---------------------------------------|
| Sap130  | 18         | Splicing | Sin3-associated Protein               |
| Esco1   | 18         | p.E524G  | N-Acetyltransferase ESCO1             |
| Pcdha9  | 18         | p.P793L  | Protocadherin a9                      |
| Nadsyn1 | 7          | p.V86A   | Glutamine-dependent NAD(+) synthetase |
| Pepd    | 7          | Splicing | Peptidase D                           |

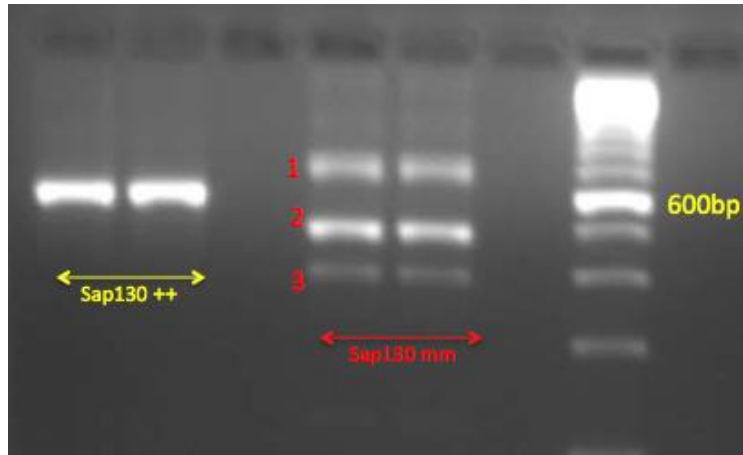


**Figure 25. Gel picture of Sap130 spliceforms in homozygous animals harvested at E12.5.**

**Homozygous animals show missing wild type band.**

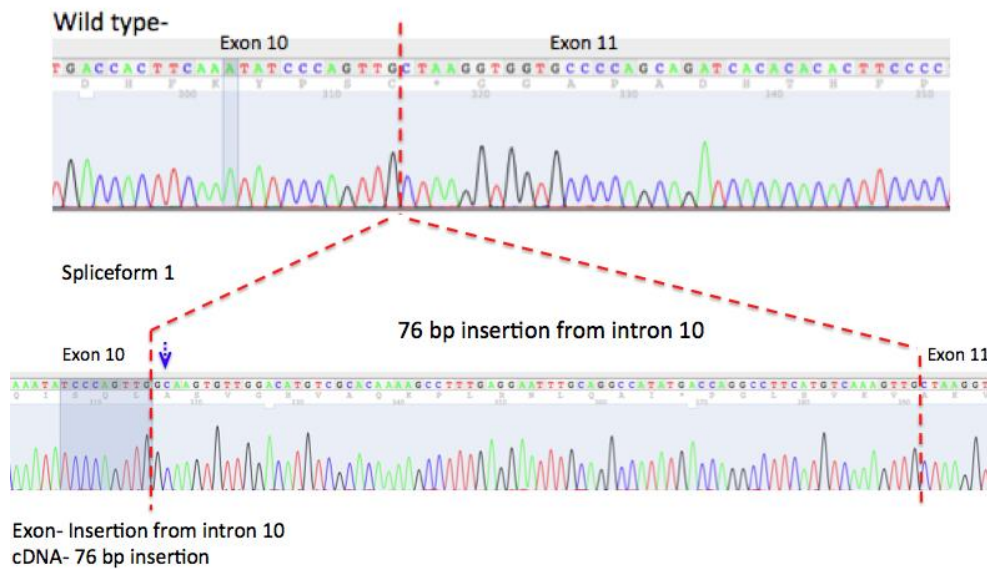


**Figure 26. Spliceform 1 of Sap130 shows 76 bp insertion in intron 10.**



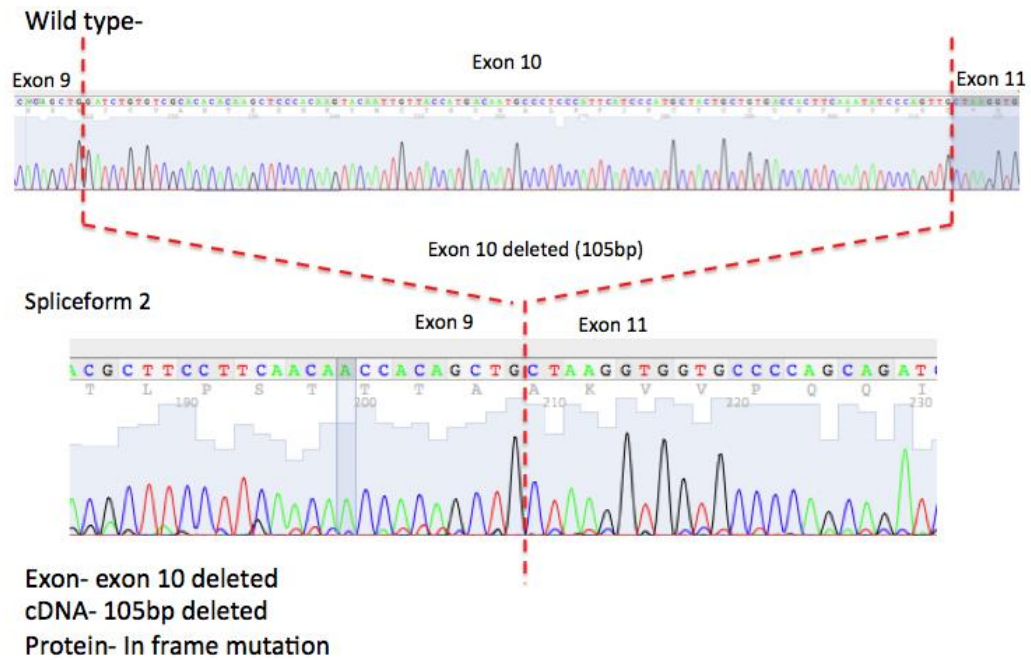


**Figure 27. Spliceform 2 in Sap130 shows in frame mutation with deletion of exon 10 (105bps).**

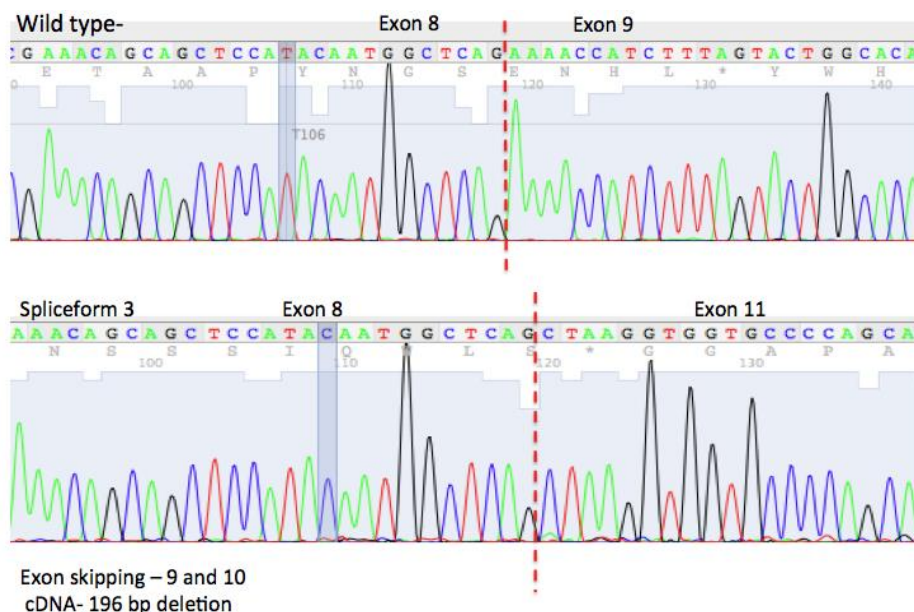


**Figure 28. Spliceform 3 in Sap130 shows skipping on exon 9 and 10.**

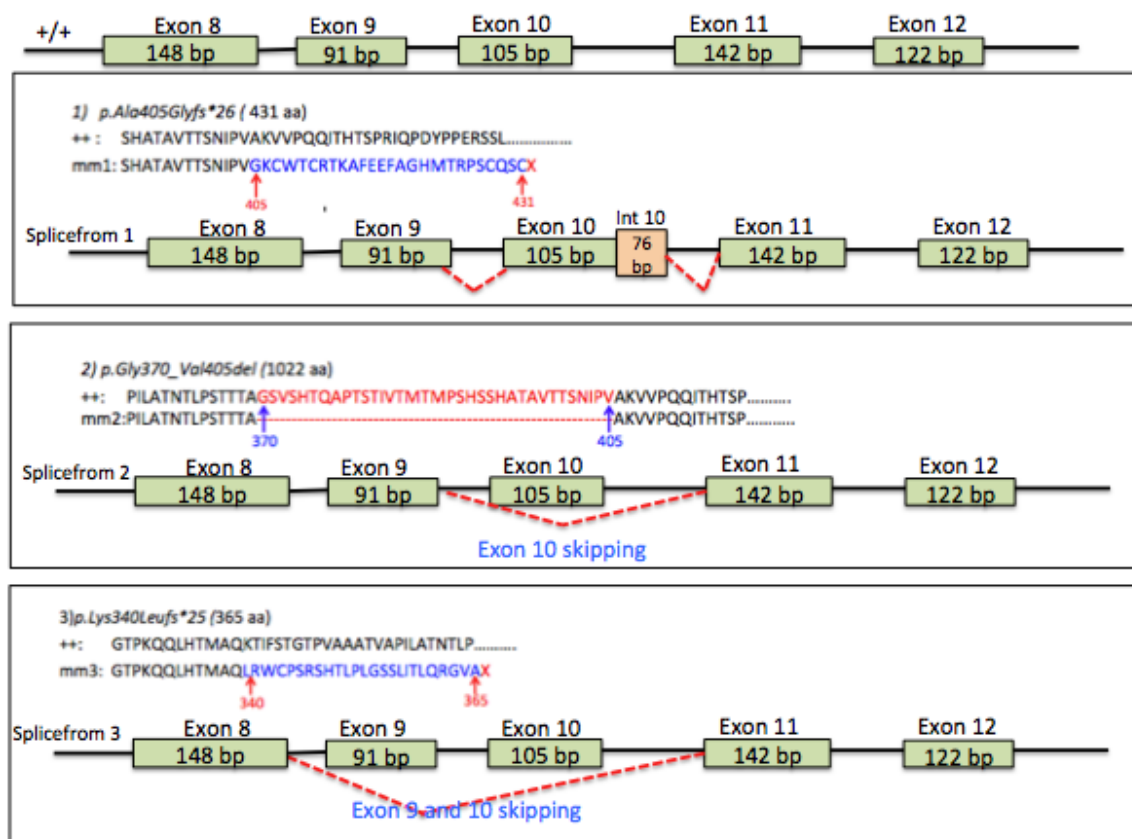


**Figure 29. Summary of three spliceforms of Sap130 in line Ohia. Spliceform 1 and 3 result in premature truncated protein.**

These five candidate genes helped us in setting up our matings for *Ohia*, and we validated our model with 15 more HLHS mutants. Interestingly in line *Ohia*, some mutants were not classical HLHS and had only a hypoplastic left heart (HLH) and a normal aortic and mitral valve. We further analyzed these 15 HLHS mutants and a total of 109 age matched littermate controls by using a decision tree analysis. (Figure 30).

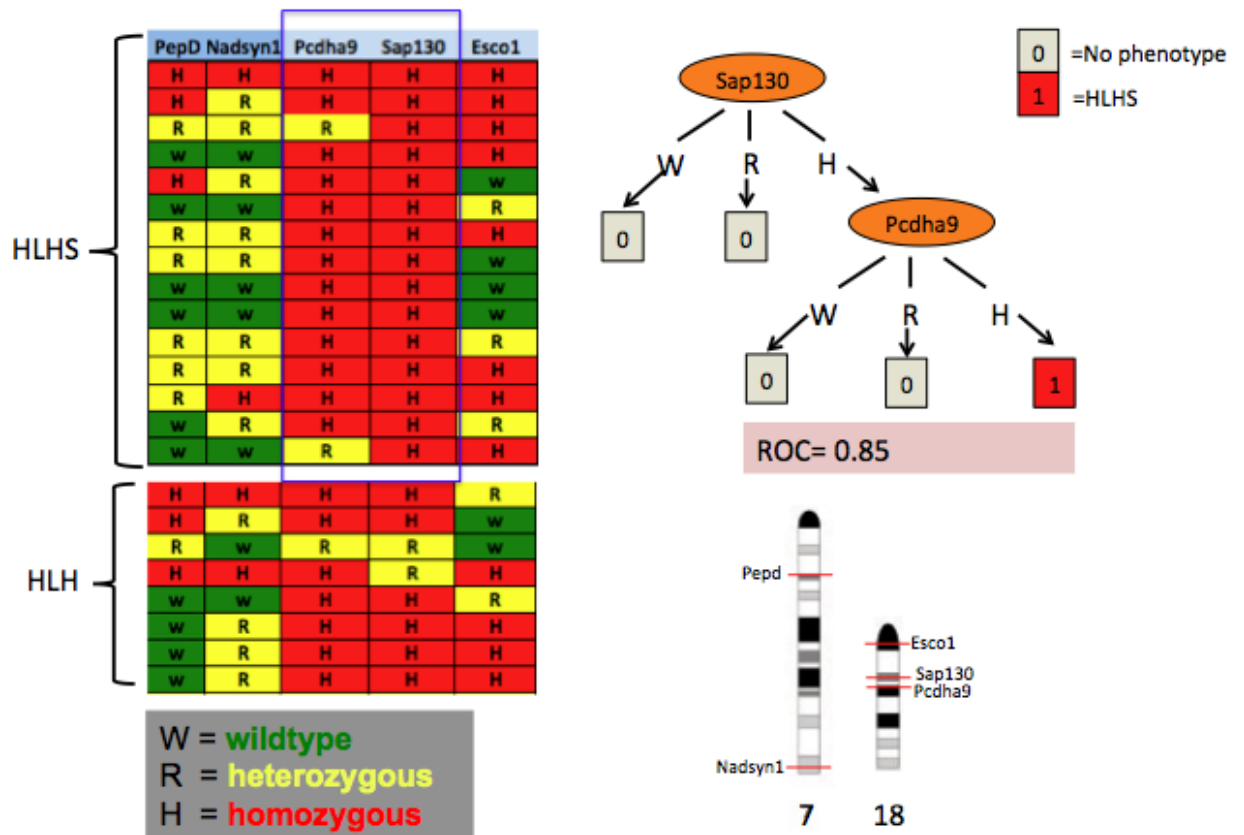


Figure 30. Genotypes of 15 HLHS mutants and 8 HLH mutants. Decision tree analysis of HLHS mutants with ROC=0.085.

Our decision tree analysis indicates that Sap130 and Pcdha9 are the two of the five genes that are probably the most important candidate genes for HLHS in line *Ohia*. A Receiver operator curve (ROC) of more than 0.5 signifies that this prediction was not random.

## 4.0 DISCUSSION

Hypoplastic left heart syndrome (HLHS), is a rare CHD. Very little is known about the genetic basis of its etiology. Our study presents the successful recovery of the first HLHS murine model. Our HLHS model in line *Ohia*, exhibits the classical cardiovascular features of HLHS along with craniofacial defects such as proboscis, absent lower jaw, low set ears, which have been previously documented in HLHS patients.

*Ohia* mutants show increased cardiomyocyte proliferation in the left ventricles at E14.5, E15.5, E16.5 and newborns. This increase in proliferation could be suggestive of defects in cell cycle regulation, which we would like to explore in our future studies. In addition, to proliferation, HLHS LV's showed increased in apoptosis. The increase in apoptosis on the left ventricle could possibly be responsible for the hypoplastic LV, but the exact mechanisms that triggers the apoptotic cascade is yet to be studied.

Our transcriptome profiling analysis from E13.5, E14.5 and E18.5 *Ohia* hearts helped us to identify 4176 differentially expressed genes. The up-regulated genes were highly enriched in pathways on cancer, focal adhesion, regulation of cytoskeleton, axon guidance, Wnt and TGF $\beta$  signaling and ECM receptor interaction, Up regulation of Wnt, TGF $\beta$  signaling and ECM receptor interaction pathways is suggestive of their role-play in the valve development [Jan-Hung Chen et al 2011] in our HLHS mutants. The up-regulated pathways encompassed several genes that were pro-apoptotic and were involved in increased cell proliferation, which validates

our findings of increased proliferation and apoptosis. Our analysis, showed the up-regulation of a number of integrins (ITGAV, ITGA3, ITGA6), which are involved in valve condensation and maturation [Borg and Terracio, 1990]

Down-regulated pathways demonstrated a global effect of mitochondrial dysfunctions, by showing perturbation in oxidative phosphorylation, Parkinson's, Huntington's and Alzheimer's disease pathways. Mitochondrial dysfunction has been well documented to play a role in CHD by inducing in utero hypoxia, loss of redox control and eventually cell death [L.Hool 2010].

Interestingly, our transcriptome analysis showed strikingly similar results as the study done by Ricc et al, 2012; using HLHS RV samples, indicating that our HLHS model indeed is a bonafide HLHS disease model.

Our whole exome data sequencing analysis has helped us to identify five candidate genes as identified from four ENU recovered mice. Further breeding has helped us to narrow our candidate genes to two genes that may be involved in the genetic etiology of HLHS in *Ohia*. Mutation in *Sap130*, a transcriptional co-repressor in Sin3A-HDAC complex, is suggestive of the involvement of chromatin remodeling in our model. Mutation in *Pcdha9* is indicative cell-adhesion and cell-migration dysfunction. This is also reflected from our transcriptome profiling, which shows enrichment of pathways of cancer, ECM-related genes, Integrins and Laminins.

Based on the findings from our study, we would hypothesize that HLHS phenotype is brought together in a piecemeal pattern. There are perturbations in genes/pathways that are responsible for the valve phenotype (eg. Integrins, TGFB and Wnt pathway, ECM maladaptation); and other pathways/genes which account for the hypoplastic LV phenotype, such as mitochondrial dysfunction, increased apoptosis in LV and increased proliferation. Chromatin remodeling probably has a more global role in the etiology of our HLHS mouse model.

## 5.0 CONCLUSION

In conclusion, we generated the first mouse model of HLHS and showed it closely models the structural heart defect and gene expression changes seen in HLHS patients. Interestingly, *Ohia* mutants also exhibited craniofacial anomalies similar to HLHS patients. Our findings suggest HLHS is accompanied by disruption of mitochondrial respiration and energy metabolism. We also see up regulation of genes involved in extracellular matrix interaction, TGFB and Wnt signaling, cell proliferation, and cell death. Genes altered in our transcriptome profile represent suggests perturbation in valve development, suggesting that the HLHS phenotype may involve valve disease. Further studies are needed to determine if the LV hypoplasia may arise downstream of improper valve development or whether it is due to cell intrinsic defects that may affect cell proliferation and cell survival. Using this mouse HLHS model, we will be able to interrogate the developmental pathways and molecular mechanism that cause HLHS.

## BIBLIOGRAPHY

- Anderson KV, Finding the genes that direct mammalian development : ENU mutagenesis in the mouse, *Trends Genet.* 2000 Mar;16(3):99-102.
- Ashleigh A Richards et al, Genetics of Congenital Heart Disease, *Curr Cardiol Rev.* 2010 May; 6(2): 91–97
- Benoit G. Bruneau, The developmental genetics of congenital heart disease. *NATURE/Vol 451/21 February 2008*
- Benson, Sharkey, Fatkin, *et al.* Reduced penetrance, variable expressivity, and genetic heterogeneity of familial atrial septal defects. *Circulation* 97, 2043-2048 (1998).
- Benson. Advances in cardiovascular genetics and embryology: role of transcription factors in congenital heart disease. *Curr Opin Pediatr* 12, 497-500 (2000).
- Bohlmeier TJ et al, Hypoplastic left heart syndrome myocytes are differentiated but possess a unique phenotype, *Cardiovasc Pathol.* 2003 Jan-Feb;12(1):23-31.
- Bruneau, B. G., Logan, M., Davis, N., Levi, T., Tabin, C. J., Seidman, J.G. and Seidman, C. E. (1999). Chamber-specific cardiac expression of Tbx5 and heart defects in Holt-Oram syndrome. *Dev. Biol.* 211,100 -108.
- Bruneau, B. G., Nemer, G., Schmitt, J. P., Charron, F., Robitaille, L., Caron, S., Conner, D. A., Gessler, M., Nemer, M., Seidman, C. E. and Seidman, J. G. (2001). A murine model of Holt-Oram syndrome defines roles of the T-box transcription factor Tbx5 in cardiogenesis and disease. *Cell* 106,709 -721
- Edward J. Hickey et al, Left Ventricular Hypoplasia A Spectrum of Disease Involving the Left Ventricular Outflow Tract, Aortic Valve, and Aorta, *Journal of the American College of Cardiology*, Vol. 59, No. 1, Suppl S, 2012
- Ferencz C. Boughman JA. Neill CA. et.al. Congenital cardiovascular malformations: questions on inheritance. Baltimore-Washington Infant Study Group. *Journal of the American College of Cardiology.* 14(3):756-63, 1989

- Gutgesell HP et al, Management of hypoplastic left heart syndrome in a consortium of university hospitals. *Am J Cardiol* 76: 809–811, 1995
- Hinton RB et al. Hypoplastic left heart syndrome is heritable. *J Am Coll Cardiol* 50: 1590–1595, 2007.
- Hiroi, Y., Kudoh, S., Monzen, K., Ikeda, Y., Yazaki, Y., Nagai, R. and Komuro, I. (2001). Tbx5 associates with Nkx2.5 and synergistically promotes cardiomyocyte differentiation. *Nat. Genet.* 28,276 -280
- Horb ME et al, Tbx5 is essential for heart development, *Development*. 1999 Apr;126(8):1739-51
- Jun K. Takeuchi et al, Tbx5 specifies the left/right ventricles and ventricular septum position during cardiogenesis, *Development* 130, 5953-5964, 2003 The Company of Biologists Ltd.
- Liberatore, C. M., Searcy-Schrick, R. D., and Yutzey, K. E. (2000). Ventricular expression of tbx5 inhibits normal heart chamber development. *Dev. Biol.* 223,169 -180
- Liu X et al, Interrogating congenital heart defects with noninvasive fetal echocardiography in a mouse forward genetic screen, *Circ Cardiovasc Imaging*. 2014 Jan 1;7(1):31-42
- Madhu Gupta et al, Transcription repression and blocks in cell cycle progression in hypoplastic left heart syndrome, *American Journal of Physiology-Heart and Circulatory Physiology*. 2008;294(5):H2268-H2275
- Marco Ricci et al, Myocardial Alternative RNA Splicing and Gene Expression Profiling in Early Stage Hypoplastic Left Heart Syndrome, *PLoS One*. 2012; 7(1): e29784
- McElhinney, Krantz, Bason, *et al.* Analysis of cardiovascular phenotype and genotype-phenotype correlation in individuals with a JAG1 mutation and/or Alagille syndrome. *Circulation* 160, 2567-2574 (2002)
- Momma, Kondo, Ando, *et al.* Tetralogy of Fallot associated with chromosome 22q11 deletion. *Am J Cardiol* 76, 618-621 (1995).
- Rosenthal J, Mangal V, Walker D, Bennett M, Mohun TJ, Lo CW. Rapid high resolution three dimensional reconstruction of embryos with episcopic fluorescence image capture. *Birth Defects Res C Embryo Today*. 2004;72:213-223
- Sedmera Det al. Current issues and perspectives in hypoplasia of the left heart. *Cardiol Young* 15: 56–72, 2005.
- Seema Mittal et al, Fetal Reprogramming and Senescence in Hypoplastic Left Heart Syndrome and in Human Pluripotent Stem Cells during Cardiac Differentiation, *The American Journal of Pathology*, Vol. 183, No. 3, September 2013



- Shokeir MH et al . Hypoplastic left heart syndrome: an autosomal recessive disorder. *Clin Genet* 2: 7–14, 1971.
- Srivastava D, Thomas T, Lin Q, Kirby ML, Brown D, Olson EN.Regulation of cardiac mesodermal and neural crest development by the bHLH transcription factor, dHAND. *Nat Genet* 1997;16:154–60
- Srivastava D. et al, HAND proteins: molecular mediators of cardiac development and congenital heart disease. *Trends Cardiovasc Med* 1999;9:11– 8.
- Yamada, M., Revelli, J. P., Eichele, G., Barron, M. and Schwartz, R. J. (2000). Expression of chick Tbx-2, Tbx-3, and Tbx-5 genes during early heart development: evidence for BMP2 induction of Tbx2. *Dev. Biol.* 228,95 -105.